



## Diatom silicon isotope ratios in Quaternary research: Where do we stand?

Patrick Frings, Virginia Panizzo, Jill Sutton, Claudia Ehlert

### ► To cite this version:

Patrick Frings, Virginia Panizzo, Jill Sutton, Claudia Ehlert. Diatom silicon isotope ratios in Quaternary research: Where do we stand?. Quaternary Science Reviews, 2024, 344, pp.108966. 10.1016/j.quascirev.2024.108966 . hal-04731623

HAL Id: hal-04731623

<https://hal.science/hal-04731623v1>

Submitted on 14 Oct 2024

**HAL** is a multi-disciplinary open access archive for the deposit and dissemination of scientific research documents, whether they are published or not. The documents may come from teaching and research institutions in France or abroad, or from public or private research centers.

L'archive ouverte pluridisciplinaire **HAL**, est destinée au dépôt et à la diffusion de documents scientifiques de niveau recherche, publiés ou non, émanant des établissements d'enseignement et de recherche français ou étrangers, des laboratoires publics ou privés.



Distributed under a Creative Commons Attribution 4.0 International License



## Diatom silicon isotope ratios in Quaternary research: Where do we stand?



Patrick J. Frings <sup>a,\*</sup>, Virginia N. Panizzo <sup>b</sup>, Jill N. Sutton <sup>c</sup>, Claudia Ehlert <sup>d</sup>

<sup>a</sup> Earth Surface Geochemistry, GFZ German Research Centre for Geosciences, Telegrafenberg, 14473, Potsdam, Germany

<sup>b</sup> School of Geography, Centre for Environmental Geochemistry, University of Nottingham, Nottingham, United Kingdom

<sup>c</sup> Univ Brest, CNRS, IRD, Ifremer, LEMAR, IUEM, F-29280, Plouzane, France

<sup>d</sup> Institute for Chemistry and Biology of the Marine Environment (ICBM), School of Mathematics and Science, Carl von Ossietzky Universität Oldenburg, Ammerländer Heerstraße 114-118, 26129, Oldenburg, Germany

### ABSTRACT

Silicon stable isotope ratios (expressed as  $\delta^{30}\text{Si}$ ) in biogenic silica have been widely used as a proxy for past and present biogeochemical cycling in both marine and lacustrine settings, in particular for nutrient utilization reconstructions. Yet an analysis of publication trends suggests a significant decline in the application of  $\delta^{30}\text{Si}$  to Quaternary science questions in the last five years. At the same time as  $\delta^{30}\text{Si}$  proxy applications have decreased, we are learning more about its complexities: an expanding body of work is highlighting biases, caveats or complications involved in the application of  $\delta^{30}\text{Si}$ -based approaches to the sediment record. These include the demonstration of species-specific silicon isotope fractionation factors (i.e. 'vital effects') or the potential for Fe or other trace metals to influence silicon isotope fractionation. Others have inferred the potential of biogenic silica dissolution to alter an initial  $\delta^{30}\text{Si}$  value, or questioned the preservation of the initial  $\delta^{30}\text{Si}$  through early diagenetic processes more generally. Another challenge receiving more attention is centered around deconvolving a  $\delta^{30}\text{Si}$ -value into a signal reflecting biological productivity and a signal reflecting changes in the  $\delta^{30}\text{Si}$  of dissolved silicon driven by whole-system and/or circulation changes. Finally, a number of studies focus on analytical difficulties, especially during sample preparation related to achieving and demonstrating a contaminant free biogenic silica. These challenges lead us to posit that the Quaternary science community is moving away from silicon isotope proxies because they are losing confidence in their reliability and usefulness. Here, focusing on the diatoms – the dominant biosilicifiers in both lakes and the ocean – we synthesize progress in understanding nuances and caveats of  $\delta^{30}\text{Si}$ -based proxies in order to answer whether the fall-off in  $\delta^{30}\text{Si}$ -based Quaternary research is warranted. We suggest that with some simple steps that can be readily implemented, and with the closing of key knowledge gaps, there is no reason to believe silicon isotopes do not have a promising future in the Quaternary sciences.

### 1. Introduction

The biogeochemical cycle of silicon (Si) in the oceans and in many lakes is dominated by silicifying organisms. These organisms extract and internally concentrate dissolved Si (dSi) from the surrounding water and use it to precipitate an amorphous hydrated silica ( $\text{SiO}_2\text{.nH}_2\text{O}$ , hereafter biogenic silica, bSi) to form their skeletons (Wallace et al., 2012). Diatoms (siliceous phytoplankton) are the principal producers of bSi in both marine and freshwater environments, but are just one of many groups with the capacity to produce bSi (Knoll, 2003). The majority of bSi is recycled, but some fraction escapes dissolution to become permanently buried in sediments (Tréguer et al., 2021). Burial of bSi represents an important sink in ocean or lake Si-budgets while simultaneously creating a biosiliceous archive of past environmental change.

In the oceans, diatoms account for ca. 40% of primary productivity (Armbrust, 2009; Nelson et al., 1995), making them a significant component of the biological pump – the suite of processes that redistributes elements from the surface to the deep ocean via the formation and sinking of particulate organic matter and biominerals (De La

Rocha, 2006). The biological pump is particularly important in determining carbon (C) distribution, meaning that understanding the modern Si cycle can shed light on the functioning of the C cycle. On millennial timescales, the variations in atmospheric  $p\text{CO}_2$  as recorded in ice-core bubbles across glacial cycles (Augustin et al., 2004) could be related to changes in the strength and efficiency of the biological pump (Harrison, 2000; Hendry and Brzezinski, 2014). On yet longer timescales, the evolutionary expansion of silicifying organisms has likely altered marine Si, C and iron (Fe) cycling (Armbrust, 2009; Maliva et al., 1989), global oxygen (O) cycling (Katz et al., 2005) and plankton macro-evolutionary trends (Lazarus et al., 2009; van Tol et al., 2012). The global rate of bSi burial may even be sought-after proxies for continental silicate-weathering rates (Frings et al., 2016; Renaudie, 2016). Similar connections can be made between freshwater Si cycling and various research fields. For example, Si availability influences lake food web structure (Sommer, 1985; Yamoah et al., 2016), ecosystem responses to eutrophication (Heathcote et al., 2015), reflects climate evolution across a range of timescales (Fortin and Gajewski, 2009; Johnson et al., 2011), and responds to lake and catchment ontogeny and

\* Corresponding author.

E-mail address: [patrick.frings@gfz-potsdam.de](mailto:patrick.frings@gfz-potsdam.de) (P.J. Frings).

human perturbations (Conley, 2002; Struyf et al., 2010). Overall, intersections of the Si cycle with different research topics provide considerable motivation for reconstructing aspects of past Si biogeochemistry across a range of timescales.

The stable isotopes of Si ( $^{28}\text{Si}$ ,  $^{29}\text{Si}$  and  $^{30}\text{Si}$ ) are a promising source of information about the past and present Si cycle (see Box 1 for a terminology glossary). For any given reaction, the ~7% mass difference between the heavier  $^{30}\text{Si}$  and the lighter  $^{28}\text{Si}$  produces different molecular dissociation energies and equilibrium partition coefficients for the isotopologues involved that translate into fractionations (Box 1) during transfers or transformations of Si (Criss, 1999). These subtle variations in Si isotope ratios (Box 1) can now be routinely determined by mass-spectrometric techniques with relatively high precision (De la Rocha, 2002; Oelze et al., 2016). In the past decade, substantial effort has been invested in producing and interpreting new  $\delta^{30}\text{Si}$  data for marine- and freshwaters (Brzezinski and Jones, 2015; Laukert et al., 2022), for water column and sediment bSi (e.g. Doering et al., 2016; Fripiat et al., 2011b; Grasse et al., 2021a), for ancient cherts (Chakrabarti et al., 2012; Tatzel et al., 2015; Ye et al., 2021), and for a suite of other pools that interact with bSi cycling (Ehlert et al., 2016; Geilert et al., 2023; Pickering et al., 2020). The issues we address in this contribution revolve around how confidently we can interpret these  $\delta^{30}\text{Si}$  values.

Interpretations of  $\delta^{30}\text{Si}$  in dSi and bSi are underlain by the discrimination against the heavier isotopes of Si during biological uptake (see details in Section 2). The process of biosilicification by various groups of organisms tends to lead to the formation of bSi that has a lower  $\delta^{30}\text{Si}$  value than the source dSi (Abelmann et al., 2015; De La Rocha et al., 1997a; Hendry and Robinson, 2012; Marron et al., 2019). Mass balance dictates that the residual dSi tends towards lower [dSi] - where the square brackets denote concentrations - and higher  $\delta^{30}\text{Si}$ , a trend that is reversed by bSi dissolution as it sinks through the water column. This gives rise to the defining characteristic of the Si cycle in the modern ocean and deep lakes, namely the gradient from low [dSi], high  $\delta^{30}\text{Si}$  surface waters to higher [dSi], lower  $\delta^{30}\text{Si}$  deep waters (Fig. 1a), though we note that lake water profiles are much scarcer (Alleman et al., 2005; Panizzo et al., 2017). Imprinted on the vertical gradient is the influence of overturning circulation, which acts to create lateral and inter-basinal [dSi] and  $\delta^{30}\text{Si}$  gradients while also resupplying dSi to the surface ocean (Fig. 1b). Physical circulation controls on the distribution of dSi also exist for lake systems, though here they tend to be related to the dynamics of seasonal stratification and mixing. Although not considered in detail here, higher plants also discriminate against the heavier isotopes of Si during phytolith formation and may also represent palaeoenvironmental archives. The key controls on lake and ocean [dSi] and  $\delta^{30}\text{Si}$  distributions are conceptually understood (e.g. de Souza et al., 2015; Vance et al., 2017), but uncertainties remain that limit our ability to find unique explanations for past and present  $\delta^{30}\text{Si}$  variations.

At a fundamental level, one issue with interpreting Si isotope data is uncertainty or variability in the suite of parameters that underpin quantitative interpretations, for example those that govern the production and dissolution of bSi or the associated Si isotope fractionations. These uncertainties are unavoidable, but how they interact and propagate, and how sensitive any given interpretation is to the underlying assumptions is rarely addressed. At a more general level, the relative importance of many of the fluxes constituting a Si budget are poorly constrained. The magnitude and  $\delta^{30}\text{Si}$  of the input fluxes are often very imprecisely known, and the output fluxes even more so (Frings et al., 2016; Rahman and Trower, 2023; Tréguer et al., 2021). This is especially true for freshwater systems, where their diversity and dynamic behaviour limit the generalisability of results from elsewhere. The quantitative impact of non-diatom groups on modern Si cycling is typically assumed to be negligible – although we know this is untrue in the modern ocean (Chu et al., 2011; Dutkiewicz et al., 2016) and in some lakes (Conley and Schelske, 1993). Understanding radiolarian or sponge effects on Si cycling necessarily assumes greater relevance as we seek to

refine Si and  $\delta^{30}\text{Si}$  budgets (Llopis Monferrer et al., 2020; Maldonado et al., 2019), especially in periods of Earth history before the rise of the diatoms. The same is true for the inorganic removal pathways of Si (Michalopoulos and Aller, 1995), which occurs via poorly understood mechanisms in the ocean (section 4) and has an essentially unexplored impact on Si cycling in lakes outside of atypical settings (Jones and Weir, 1983). At steady-state, mean lake or ocean  $\delta^{30}\text{Si}$  should be offset from the mean  $\delta^{30}\text{Si}$  of the input Si fluxes by an amount corresponding to the net fractionation associated with the formation and burial of biogenic Si. But how can we distinguish between  $\delta^{30}\text{Si}$  changes driven by processes within the system, and those reflecting a transient adjustment to external (i.e. continental/catchment) forcing (Section 5)? Overall, these issues mean we lack a firm foundation for confidently ascribing interpretations to  $\delta^{30}\text{Si}$  variations in both the recent and geological past.

### 1.1. Are silicon isotopes going out of fashion?

The so-called ‘Elderfield proxy curve’ (Chase et al., 2018; Elderfield, 2002) provides an irreverent view of the evolution of confidence in a given palaeoproxy. It recognizes three phases: an initial period of optimism with simple relationships between environmental driver and proxy response, a crash into pessimism as the complexities of the proxies become clearer, and a final plateau of realism where the nuances and caveats of proxy application are better understood. Fig. 2 shows an analysis of publication trends (limited to marine environments due to the larger number of papers) over the past two decades that suggests we might be deep in the valley of pessimism regarding the application of Si isotopes to Quaternary science questions. The first impactful application of Si isotopes to Quaternary science questions was the seminal work of De La Rocha and colleagues towards the end of the 1990’s (De La Rocha et al., 1996, 1997b, 1998, 2000). With the increased availability of multi-collector ICP-MS from the early 2000’s, an average of 2.8 Quaternary focused papers per year were published with Si isotopes as a central focus. In the years 2018–2023, to the best of our knowledge, there have been only five Quaternary-focused applications of  $\delta^{30}\text{Si}$  to the marine realm in total (i.e., Dumont et al., 2020; Hendry et al., 2021; Pichevin et al., 2020; Snelling et al., 2022; Worre et al., 2022). The freshwater realm tells a similar story: Street-Perrott and colleagues pioneered lacustrine applications of Si isotopes (Street-Perrott and Barker, 2008; Street-Perrott et al., 2008), but with notable exceptions (Xiang et al., 2023) there has been a drop-off in palaeolimnological applications in recent years. In contrast to the decline in palaeo-applications, the number of papers exploring the complexities of modern-day Si cycling is accelerating. These papers touch on topics including fractionation (Doering et al., 2021; Grasse et al., 2021b), diagenesis (Luo et al., 2022; Ward et al., 2022a), and ocean or lake Si budgets (Hatton et al., 2023; Rahman and Trower, 2023; Zahajská et al., 2021). Is there a link between these two contrasting publication trends? In other words, as we learn more about the complexities of modern-day Si (isotope) cycling, do we become more pessimistic about palaeo-applications?

The purpose of this contribution is to review the processes and parameters that introduce uncertainty to reconstructions in order to assess whether the pessimism is reasonable. With this completed, we identify pathways towards more realistic and well-grounded applications of Si isotopes to questions in the Quaternary and deeper times. Throughout, we draw on literature for both marine and lacustrine records, highlighting similarities and differences where necessary. Our goal is not to recapitulate all previous work – which is already reviewed to various extents elsewhere (Farmer et al., 2021; Sutton et al., 2018a; Tréguer et al., 2021). Instead, we explore what may be driving the decline in  $\delta^{30}\text{Si}$ -based Quaternary research (Fig. 2), question whether the decline is warranted, and provide recommendations for future work.

**Box 1**

Glossary of relevant terminology

**Isotope ratio notation.**

**R:** The **isotope ratio** is the fundamental quantity in isotope (bio)geochemistry and is the dimensionless number obtained when the number of atoms of one isotope in a given phase is divided by the number of atoms of another isotope of the same element in the same phase. For example, a silicon isotope ratio in phase A may be defined as  $R = N(^{30}\text{Si})_A/N(^{28}\text{Si})_A$ , where  $N$  is the number atoms of the  $^{30}\text{Si}$  or  $^{28}\text{Si}$  isotope.

**$\alpha$  ('alpha')**: alpha notation is a dimensionless quantity used for an **isotope fractionation factor**, defined as a ratio of ratios. For example,  $\alpha^{30/28}\text{Si}_{A/B} = R(^{30}\text{Si}/^{28}\text{Si})_A/R(^{30}\text{Si}/^{28}\text{Si})_B$  encapsulates the change in ratio expected.

**$\delta$  ('delta')**: delta is a dimensionless number used to express a **relative isotope-ratio difference**, i.e. the deviation in a given ratio (e.g.  $^{30}\text{Si}/^{28}\text{Si}$ ) in one phase relative to another. For Si, delta values are almost exclusively given as the deviation of a sample ratio from the same ratio in the internationally accepted zero-point of the silicon isotope scale, i.e. NBS28 quartz sand (NIST SRM 8546). A  $\delta$ -value for phase A is thus defined as  $\delta^{30/28}\text{Si}_{A/\text{NBS28}} = R(^{30}\text{Si}/^{28}\text{Si})_A/R(^{30}\text{Si}/^{28}\text{Si})_{\text{NBS28}} - 1$ , where similar formulations can be written for the ratios  $^{29}\text{Si}/^{28}\text{Si}$  or even  $^{30}\text{Si}/^{29}\text{Si}$  (by convention the heavier isotope is in the numerator). For simplicity, the subscripts and denominator isotope are typically omitted, leaving just  $\delta^{30}\text{Si}$  or  $\delta^{29}\text{Si}$  as the reported notation. Expressions defining  $\delta$ -values including a factor of 1000 are commonly found in the literature and are strictly incorrect, since the permil symbol (‰) already implies a factor of 1000.

**$\Delta$  ('big-delta')**: big delta notation is used to express an **isotope difference**, i.e. the numerical difference between two  $\delta$ -values for phases A and B. For example,  $\Delta^{30/28}\text{Si}_{A/B} = \delta^{30/28}\text{Si}_A - \delta^{30/28}\text{Si}_B$ . Note that  $\Delta$  is used in other communities to refer to deviation from a reference line in three-isotope space.

**$\epsilon$  ('epsilon')**: epsilon is defined as  $\alpha - 1$  and is commonly reported in permil. It is commonly referred to as an **isotope fractionation** or an **isotope enrichment factor**, with the first term being preferred. Note that  $\epsilon$  is used in other communities analogously to a  $\delta$ -value, but in parts per 10000 rather than parts per thousand (i.e. permil).

The alpha, delta and epsilon notations are in principle interchangeable.

**Fractionation:** A discrimination of one isotope relative to another during a biological, chemical or physical process. Most fractionations are **mass-dependent**, i.e. the discrimination is due to subtle differences in biogeochemical behaviour induced by differences in isotope mass. This means that  $\delta^{30}\text{Si}$  and  $\delta^{29}\text{Si}$  values are readily convertible to each other, convenient for early work that did not report  $^{30}\text{Si}/^{28}\text{Si}$  ratios.

**Kinetic isotope effect:** a partitioning of isotopes during a unidirectional or irreversible process due to the effect of an isotope substitution on a rate constant or diffusion constant. Kinetic isotope effects almost always favour the transfer of the lighter isotopes to the product. Kinetic isotope effects can be **primary** if the isotope substitution involves bond creation or breaking during a reaction, or **secondary** if the isotope substitution is elsewhere on the isotopologue.

**Equilibrium isotope effect:** a partitioning of isotopes between two co-existing phases at chemical equilibrium that reflects the effect of isotope substitution on an equilibrium constant. Equilibrium isotope effects tend to favour the heavier isotopes partitioning into the stronger bonds, which is not always trivial to assess.

**Silicon biogeochemistry terminology.**

**Diatoms:** Unicellular autotrophic algae of class Bacillariophyceae found in all aquatic environments. Diatoms form a cell wall comprised of amorphous silica known as a frustule and today represent the most important biological component of the marine and most freshwater silicon cycles. They have their evolutionary roots in the Mesozoic, though molecular clock and fossil evidence yield inconsistent timings of emergence.

**Radiolarians:** Unicellular heterotrophic (occasionally with symbionts) protozoa found throughout the entire water column of the ocean. They belong to supergroup Rhizaria – making them a sister lineage to the calcifying protozoa foraminifera – and taxa within class Polycystinea produce intricate siliceous skeletons termed tests. Radiolarians expanded in the Cambrian and Ordovician, and often function as important biostratigraphic marker fossils.

**Sponges:** Benthic organisms belonging to the phylum Porifera. Four classes of sponges are recognized, of which three (Hexactinellida, Demospongidae and Homoscleromorpha) produce siliceous skeletons predominantly comprised of needle-like structures known as spicules. Demospongidae includes both marine and freshwater taxa, though marine species are much more diverse and well-studied. Sponges have their roots in the late Precambrian, likely making them the first ecologically important biosilicifiers.

**Dissolved Si (dSi):** dSi refers to silicon present as a solute. In most Earth surface environments, dSi is found as the undissociated monomeric silicic acid  $\text{H}_4\text{SiO}_4$ , though at higher pH the deprotonated forms  $\text{H}_3\text{SiO}_4^-$  and  $\text{H}_2\text{SiO}_4^{2-}$  species are also found (at 25 °C,  $\text{pK}_{\text{a}1} \approx 9.84$ ;  $\text{pK}_{\text{a}2} \approx 13.2$ ). At higher concentrations, polymeric Si species can occur. Here, we use square brackets (i.e.  $[\text{dSi}]$ ) to indicate a molar concentration. dSi concentrations in the literature are also reported in mass units for both elemental Si ( $M_R = 28.086 \text{ g mol}^{-1}$ ) and molecular  $\text{SiO}_2$  ( $M_R = 60.084 \text{ g mol}^{-1}$ ).

**Biogenic silica (bSi):** The form of solid silica produced by diatoms, radiolarians, sponges and other biosilicifiers that have the capacity to take dSi from the surrounding water, concentrate it and guide its deposition into often incredibly intricate structures. bSi (also called opal in the literature) is an X-ray amorphous, hydrated silica with similar properties to inorganic amorphous silica/opal.

**Diagenesis:** The suite of processes that govern the preservation of a solid, and can modify its structural or chemical composition, after its deposition in lake or ocean sediments, often driven by changes in physical (e.g. temperature or pressure) and biogeochemical (e.g. porewater solute composition, microbial activity) conditions in the sediments.

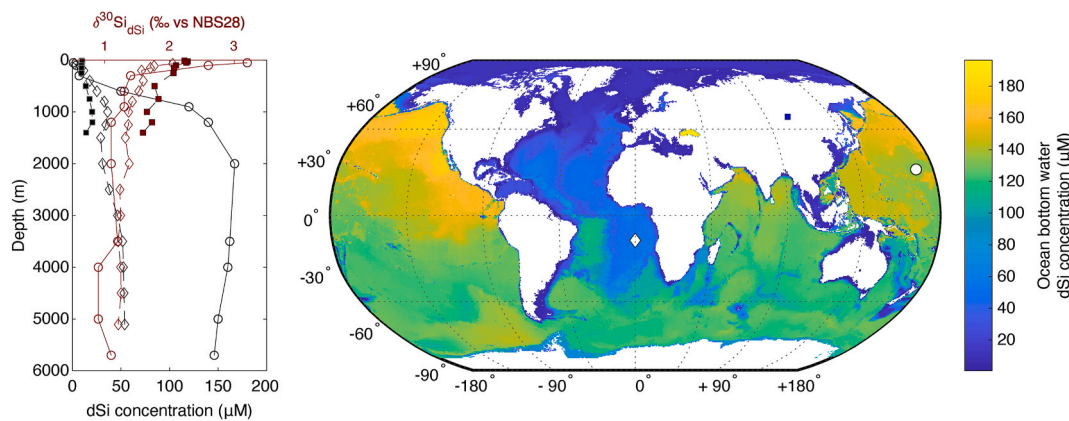


**Fig. 1.** Key vertical and lateral gradients in the modern ocean Si cycle. A: Vertical profiles in Si concentrations (black lines) and dissolved Si  $\delta^{30}\text{Si}$  (red lines) from the Equatorial Atlantic (diamonds), North Pacific (circles) and Lake Baikal (filled squares) exhibit typical ‘nutrient-like’ distributions, i.e. controlled by the production of biomass in the euphotic zone and its progressive dissolution during sinking. Data from de Souza et al. (2012b) and Reynolds et al. (2006) for the Atlantic and Pacific profiles, respectively, and from Panizzo et al. (2017) for Lake Baikal. B: Ocean bottom water dissolved Si concentrations, with low North Atlantic [dSi] and higher North Pacific [dSi], following the general trend of water mass age. Symbols correspond to the location of data in panel A. Data from the WOCE Global Hydrographic Climatology (Gouretski and Koltermann, 2004).

## 2. Silicon isotopes in diatoms as palaeoproxies: the principles

The first – and still most widely applied – use of diatom  $\delta^{30}\text{Si}$  was as a proxy for primary productivity. This is underpinned by the observation that diatoms (and other biosilicifiers) fractionate Si isotopes during biosilicification (De La Rocha et al., 1997a; Sutton et al., 2018a). The fundamental principle is encapsulated in simple mass-balance models of the kind shown in Fig. 3 (Varela et al., 2004). In brief, as diatoms progressively deplete the available dSi, both their frustules and the residual dSi trend towards higher  $\delta^{30}\text{Si}$  signatures (Fig. 3a and b). At close to zero utilization of the available dSi, diatom  $\delta^{30}\text{Si}$  will be offset by one fractionation from the source dSi  $\delta^{30}\text{Si}$ , while at 100% utilization of the available dSi, mass-balance requires that diatom  $\delta^{30}\text{Si}$  is equivalent to the source dSi. Diatom  $\delta^{30}\text{Si}$  is therefore related to *relative* utilization of the available dSi, rather than primary productivity in an *absolute* sense. In principle, this conceptual framework yields a potential range of diatom  $\delta^{30}\text{Si}$  equivalent in magnitude to the fractionation associated with diatom biosilicification. Two endmember models are commonly employed, though the terminology is often inconsistent. The first – which we call the ‘steady state’ model – relates diatom  $\delta^{30}\text{Si}$  to the relative utilization of dSi as (solid lines in Fig. 3b):

$$\delta^{30}\text{Si}_{\text{diatom}} = \delta^{30}\text{Si}_{\text{source}} + (1 - f_{\text{Si}})\epsilon_{\text{diatom}}^{30} \quad \text{Eqn. 1}$$

And the  $\delta^{30}\text{Si}$  of the residual water as:

$$\delta^{30}\text{Si}_{\text{residual}} = \delta^{30}\text{Si}_{\text{source}} - f_{\text{Si}}\epsilon_{\text{diatom}}^{30} \quad \text{Eqn. 2}$$

Where  $\epsilon_{\text{diatom}}^{30}$  is the fractionation (in permil; see Box 1) associated with diatom growth, and  $f_{\text{Si}}$  is the fractional utilization of dSi for diatom growth (i.e.  $f_{\text{Si}} = 0$  implies no dSi uptake, and  $f_{\text{Si}} = 1$  implies total conversion of dSi to bSi). Implicit in the steady state model is the idea that the system under consideration is open with respect to ‘new’ dSi (typically invoked as upwelling) and that diatom growth converts a consistent fraction (i.e.  $f_{\text{Si}}$ ) of this to bSi.

The second endmember model – a Rayleigh distillation model – relates  $\delta^{30}\text{Si}_{\text{diatom}}$  to  $f_{\text{Si}}$  as (dotted line in Fig. 3b):

$$\delta^{30}\text{Si}_{\text{diatom}} = \delta^{30}\text{Si}_{\text{source}} - \epsilon_{\text{diatom}}^{30} \cdot \left( \frac{(1 - f_{\text{Si}})\ln(1 - f_{\text{Si}})}{f_{\text{Si}}} \right) \quad \text{Eqn. 3}$$

And the residual dSi as (dashed line in Fig. 3b):

$$\delta^{30}\text{Si}_{\text{residual}} = \delta^{30}\text{Si}_{\text{source}} + \epsilon_{\text{diatom}}^{30} \cdot \ln(1 - f_{\text{Si}}) \quad \text{Eqn. 4}$$

Implicit in the Rayleigh model is the assumption that the source pool

of dSi is isolated from new supply that is progressively depleted over the course of a bloom or growing season (i.e.  $f_{\text{Si}}$  increases monotonically), and that there is no significant back-reaction (i.e. dissolution). Eqn. (3) provides an estimate of the accumulated diatom pool, i.e. integrated over the progression from  $f_{\text{Si}} = 0$  to the final  $f_{\text{Si}}$  value before growth ends or new dSi supply begins; the instantaneous diatom  $\delta^{30}\text{Si}$  produced at some timepoint is simply the residual dSi  $\delta^{30}\text{Si}$  (Eqn. (4)) plus a fractionation  $\epsilon_{\text{diatom}}^{30}$ . The progressive depletion yields the characteristically curved lines in Fig. 3b and provides a mechanism to achieve high residual dSi  $\delta^{30}\text{Si}$  values, such as those of up to +4.4‰ seen in dSi-deplete regions of the Pacific (Grasse et al., 2013, 2020), otherwise unattainable with a ‘steady-state’ model. Despite the differences in predictions for how the residual dSi should evolve as a function of  $f_{\text{Si}}$ , the two frameworks are fairly similar in their prediction of mean diatom  $\delta^{30}\text{Si}$  (Fig. 3b), which is fortuitous for palaeo-applications.

Both the steady-state and Rayleigh models are oversimplifications, but even from the mass-balances given in Eqns (1)–(4) we can identify two parameters that must be known if diatom  $\delta^{30}\text{Si}$  is to be interpreted in terms of relative productivity, i.e.  $f_{\text{Si}}$ . The first is  $\epsilon_{\text{diatom}}^{30}$ , i.e. the silicon isotope fractionation associated with diatom growth: implicit in most applications of diatom  $\delta^{30}\text{Si}$  as a palaeoproduction proxy is the assumption that the fractionation associated with silicification is constant (discussed in Section 3). The second parameter is the  $\delta^{30}\text{Si}_{\text{source}}$  term: both the steady-state and Rayleigh model assume this is known, and constant (discussed in Section 5). An implicit assumption not directly captured in Eqns (1)–(4) is the requirement that once set, diatom  $\delta^{30}\text{Si}$  is not changed during sinking and burial (discussed in Section 4). A final interpretative choice relates to the decision between applying a steady-state (Eqns (1) and (2)), Rayleigh (Eqns (3) and (4)) or another framework. Overall, several assumptions need to be valid for these Si isotope proxies to work. These assumptions are not necessarily trivial to validate in the modern world and become correspondingly more uncertain in the past (Fripiat et al., 2012). In this contribution we synthesize mechanistic understanding of the processes that may affect these assumptions.

### 2.1. Other biosiliceous archives of marine and lacustrine palaeoenvironments

Other major groups of biosilicifiers (sponges and radiolarians; see Box 1) are also increasingly being used for palaeoenvironmental inferences but are less firmly established. We only briefly summarize the basics of their interpretation here. In the case of the sponges, their

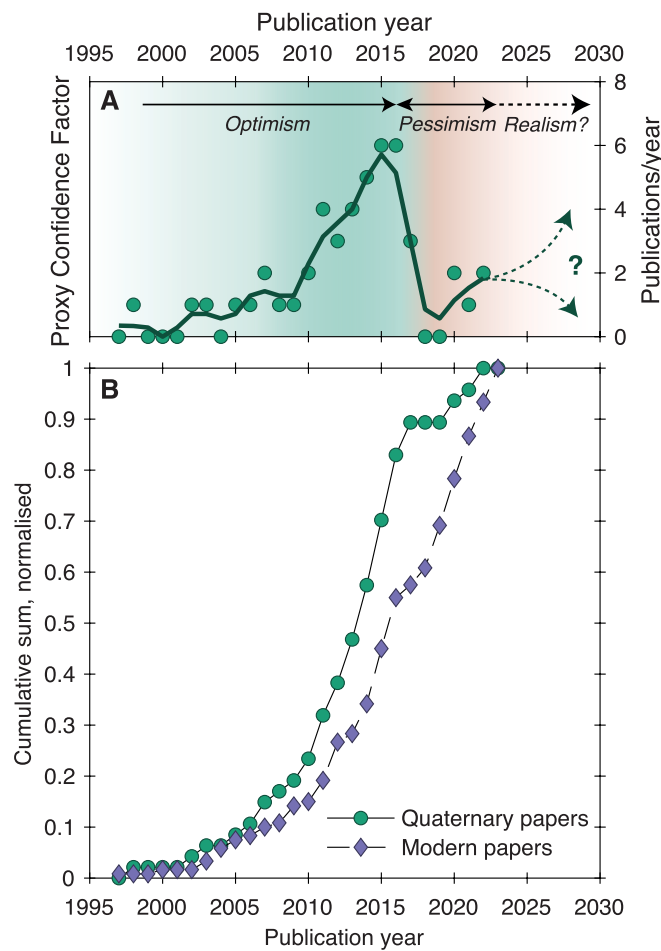


**Fig. 2.** Quaternary applications of Si isotopes appear to follow the ‘Elderfield Curve’ of proxy scientific maturation (Chase et al., 2018; Elderfield, 2002) where initial optimism is broken by a period of despair, before a more nuanced – and realistic – understanding of proxy behaviour is obtained. A: Number of publications with a Quaternary and marine focus per year, from 1997 to 2024. B: Cumulative publication rate of papers with a Quaternary focus (green circles, total = 47) or a modern marine focus (purple diamonds, total = 120); modern papers that improve understanding of, or add complexity to, marine Si cycling are accelerating in publication rate while palaeo-applications have stalled. Paper counts are based on a Web of Science query in February 2024 (search query: ALL=(“silicon isotop\*” OR “Si isotop\*” OR “d30Si” OR “630Si” OR “delta(30)Si” OR “delta(30) Si” OR “delta Si-30”), returning 1087 records that were subsequently manually classified). Given the larger sample size, this analysis is restricted to papers with a marine focus.

application of Si isotope geochemistry is underpinned by the observation that Si isotope fractionation during sponge silicification is not constant, but instead dependent on ambient dSi concentrations (Fig. 3C; Cassarino et al., 2018; De La Rocha, 2003; Hendry and Robinson, 2012; Wille et al., 2010b). A relationship observed in living and core-top samples across a range of marine environments (Cassarino et al., 2018; Hendry et al., 2019; Hendry and Robinson, 2012) demonstrates that at low (<10  $\mu\text{M}$ ) dSi concentrations sponge Si isotope fractionation is ca.  $-1\text{\textperthousand}$ , plateauing to a value of ca.  $-6\text{\textperthousand}$  at higher concentrations (>150  $\mu\text{M}$ ) (Fig. 3c). This makes sponges recorders of palaeo-dSi, and by extension gives them utility as water-mass tracers and circulation proxies (cf. Fig. 1B). The third major group of biosilicifiers in the modern ocean – radiolarians – produce siliceous tests with a  $\delta^{30}\text{Si}$  value that is offset from seawater dSi by a small magnitude fractionation that might be weakly dependent on dSi concentration (Doering et al., 2021). Here, the interpretative framework is less developed but the general principle is that they are not sufficiently productive to change seawater dSi

concentration or  $\delta^{30}\text{Si}$ , and as such their  $\delta^{30}\text{Si}$  values passively record that of the depth in the water column where they obtain their dSi.

Given the less developed state of sponge- and radiolarian-based proxies, we focus in this contribution on the diatoms, but note that many issues we discuss below (variability in fractionation factors; Section 3), post depositional alteration (Section 4), uncertainty in source pool dSi composition (Section 5) and practical analytical issues (Section 6) are not unique to the diatoms, but applicable to *all* siliceous organisms.

### 3. The influence of variable silicon isotope fractionation by diatoms

As described above, diatoms take up Si from their surrounding water during the formation of their silica frustules and a kinetic isotope fractionation (Box 1) occurs because the different Si isotopes have slightly different rate constants during dissolved Si uptake and polymerization (Cassarino et al., 2021). This isotope fractionation can potentially be influenced by the specific transport proteins and enzymes involved in Si uptake by diatoms and temperature of the surrounding water (Sutton et al., 2018a). Intracellular processes, including the polymerization of silica, silica deposition, and any dSi efflux, will also contribute to the net Si isotope fractionation (Milligan et al., 2004), though these are difficult to isolate (Cassarino et al., 2021). The first quantification of diatom Si isotope fractionation (De La Rocha et al., 1997a) yielded a fractionation ( $\varepsilon_{\text{diatom}}^{30}$ ) of  $-1.1 \pm 0.4\text{\textperthousand}$ , a value that continues to be cited today. Since then, several studies (including both *in vitro* and *in situ* experiments and observation-based approaches) have examined the potential factors influencing the variability in diatom Si isotope fractionation and its potential impact on palaeo-interpretations. Fig. 4 shows a compilation of the various determinants of diatom Si isotope fractionation from published studies that are discussed in the sections below.

#### 3.1. In vitro experiments

To our knowledge, *in vitro* studies have focused almost exclusively on marine diatom species, with Sun et al. (2014) presenting an exception for two estuarine taxa. Under optimized growing conditions and in a controlled laboratory environment, species-dependent Si isotope fractionation (occasionally termed ‘vital effects’ and denoted as  $\varepsilon_{\text{diatom}}^{30}$ ; see Box 1), by marine diatoms was observed by Sutton et al. (2013). Moving beyond earlier work that inferred or assumed an invariant  $\varepsilon_{\text{diatom}}^{30}$  (De La Rocha et al., 1997b; Milligan et al., 2004), they demonstrated a range of  $\varepsilon_{\text{diatom}}^{30}$  between at least  $-2.09\text{\textperthousand}$  to  $-0.53\text{\textperthousand}$ , leading Sutton et al. (2013) to recommend that reconstructions using the  $\delta^{30}\text{Si}$  of diatoms as a Si utilization proxy should also determine the species composition of the samples analysed. The experiments of Sutton et al. (2013) did not yield conclusive results regarding the factors controlling  $\varepsilon_{\text{diatom}}^{30}$ , but they suggested it may be influenced by temperature, [dSi], or other variables influencing the processes of, and balance between, Si uptake and polymerization, but any phylogenetic, morphological, physiological or environmental conditions (e.g. strain, temperature, growth, Si deposition) influencing diatom Si isotope fractionation have been challenging to identify. Cassarino et al. (2021) presented an experiment designed to reproduce diatom intracellular silica precipitation, and show that biomimetic molecules had little influence on the magnitude of fractionation, implying the parameters that govern the magnitude of Si isotope fractionation in abiotic systems (see section 4.4) may also apply to biosilicification. Across the range of all studies on marine taxa in Fig. 4, there is no significant relationship between [dSi] and the magnitude of fractionation ( $r^2 = 0.01$ ,  $p > 0.05$ ,  $n = 112$ ). Meyerink et al. (2017) were able to demonstrate decreased Fe bioavailability increases the magnitude of  $\varepsilon_{\text{diatom}}^{30}$  (towards more negative values) for *Proboscia inermis* and *Eucampia antarctica* by ca.  $0.2\text{\textperthousand}$  in culture experiments, sparking interest in understanding the mechanisms affecting  $\varepsilon_{\text{diatom}}^{30}$  in these organisms.

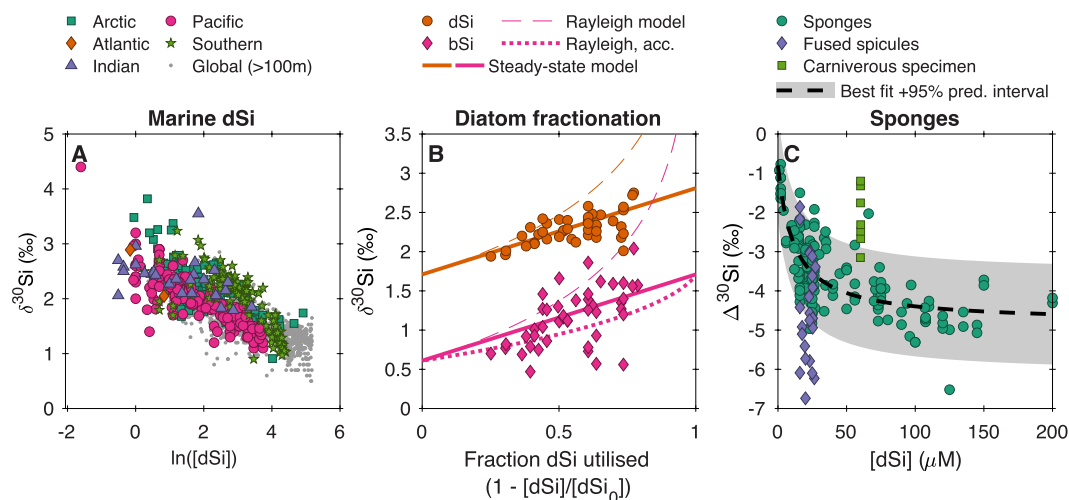


**Fig. 3.** The empirical underpinnings of Si isotope proxies. A: Compilation of published ocean dSi  $\delta^{30}\text{Si}$  data with emphasis on euphotic zone (<100 m depth; coloured symbols) showing the general negative relationship between  $[\text{dSi}]$  and  $\delta^{30}\text{Si}$  reflecting the Si isotope fractionation associated with removal of dSi by the diatoms and other biosilicifiers B: Data from Closset et al. (2016) (all samples from the KEOPS-1 cruise in the upper 100 m) and lines showing the predictions of the ‘steady-state’ (Eqns (1) and (2)) and ‘Rayleigh’ (Eqns (3) and (4)) models with  $\delta^{30}\text{Si}_{\text{source}} = 1.71$  and  $\varepsilon_{\text{diatom}}^{30} = -1.2\text{‰}$ . C: Compilation of sponge Si isotope fractionation, expressed as  $\Delta^{30}\text{Si} = \delta^{30}\text{Si}_{\text{dSi}} - \delta^{30}\text{Si}_{\text{sponge}}$  (see Box 1), as a function of ambient dissolved Si concentrations. Data from (Cassarino et al., 2018; Hendry et al., 2010; Hendry and Robinson, 2012; Wille et al., 2010a) with a best-fit line and 95% prediction intervals of the form  $\Delta^{30}\text{Si} = a + b/(c + [\text{dSi}])$  shown following e.g. Hendry and Robinson (2012 and discussion therein). ‘Fused’ spicules (i.e. those assigned a category of F2–F5) from Cassarino et al. (2018) and data from the hypersilicified, carnivorous sponge *Asbestopluma* from Hendry et al. (2015) are shown for comparison but excluded from the fit, analogous to how certain diatom taxa exhibit unusual Si isotope fractionations (see section 3). Panel A data from (Beucher et al., 2008, 2011; Cao et al., 2012; Cardinal et al., 2005; Closset et al., 2016; Coffineau et al., 2014; De La Rocha et al., 2000; de Souza et al., 2012a, 2012b; Debry et al., 2022; Ehlert et al., 2012; Fripiat et al., 2011b; Grasse et al., 2013, 2021a; Laukert et al., 2022; Singh et al., 2015; Sutton et al., 2018b; Varela et al., 2004, 2016).

Pichevin et al. (2014) demonstrated that elevated export of bSi relative to organic C, and a higher rate of bSi burial in some ocean upwelling zones were linked to Fe limitation. This follows from a well-documented increase in diatom silicification and  $\text{Si}/\text{NO}_3^-$  uptake stoichiometry under Fe limiting conditions (Takeda, 1998), an observation that underpins the ‘Silicic Acid Leakage Hypothesis’ (SALH). Pichevin et al. (2014) suggested that the lower  $\delta^{30}\text{Si}$  signature of diatoms during glacial stage Heinrich events supported the idea that the organisms had a lower requirement for dSi due to it coinciding with more Fe replete conditions driven by enhanced glacial dust delivery in stadials (Matsumoto et al., 2002). This argument was supported by the application of the closed Rayleigh isotope model (Section 2; De La Rocha et al., 1997a). However, the data from Meyerink et al. (2017) complicate this interpretation, given that the  $\delta^{30}\text{Si}$  values of diatoms from the laboratory cultures were lower under Fe-deplete conditions. Devi (2023) also suggested that other trace elements, such as cobalt (Co), can influence the  $\varepsilon_{\text{diatom}}^{30}$  of diatoms. However, it is important to highlight that research on the interactions between trace elements such as Co and Si isotope fractionation in diatoms is a relatively emerging field, and more studies are needed to elucidate the specific mechanisms involved. Clearly, more work is needed to understand the mechanisms and processes influencing the differences that are observed *in vitro*.

Other silicifying organisms, including the sponges (Fig. 3c), polycystine radiolarians, and choanoflagellates typically have lower  $\delta^{30}\text{Si}$  signatures compared to diatoms (Egan et al., 2012; Hendry et al., 2010; Marron et al., 2019; Wille et al., 2010a), supporting the suggestion that different silicification mechanisms can be a governing factor in the observed differences in  $\varepsilon_{\text{diatom}}^{30}$  (Cassarino et al., 2018; Doering et al., 2021). In addition, diatoms from the genus *Chaetoceros*, which produces long siliceous setae after cell division, were shown to have a significantly larger magnitude  $\varepsilon_{\text{diatom}}^{30}$  (i.e.  $-1\text{‰}$  to  $-2\text{‰}$ ) than the other species grown under laboratory-controlled conditions, suggesting that their two-step biomineralization process may influence their  $\delta^{30}\text{Si}$  (Devi, 2023; Sutton et al., 2013). No data are yet available regarding the  $\delta^{30}\text{Si}$  of resting spores of *Chaetoceros*, or any other species, but given their

abundance in the palaeorecord their presence may bias the  $\delta^{30}\text{Si}$  in bulk diatom samples (see Section 6 for more details).

### 3.2. In situ observations

The Si isotope fractionation (here sometimes denoted as  $\varepsilon_{\text{diatom}}^{30}$  and sometimes described as  $\Delta^{30}\text{Si}$ ; Box 1), observed in modern field studies does not appear to vary solely as a function of species composition (Fig. 4). The field observations highlight that other factors besides species composition influence  $\varepsilon_{\text{diatom}}^{30}$ . In the Southern Ocean, where most marine studies have been conducted, the  $\delta^{30}\text{Si}$  of diatoms show latitudinal differences (Closset et al., 2015; Fripiat et al., 2012; Varela et al., 2004). Part of this range is likely due to the changes in the  $\delta^{30}\text{Si}$  of the source waters and relative Si utilization by diatoms. The extent to which differences in the species assemblage compositions play a role is unclear because most studies do not report the assemblage composition. A recent study approximating the Si isotope fractionation of freshwater diatoms as the Si isotope difference between bSi from plankton tows or surface scrape, and contemporaneous dSi samples, does appear to be influenced by species assemblage composition (Schmidtbauer et al., 2022). The authors speculated that the largest magnitude fractionation they observed ( $\Delta^{30}\text{Si} = -3.9\text{‰}$  for a *Fragilaria* dominated assemblage) might reflect trace-metal abundance in the hydrothermally influenced systems studied. In contrast,  $\varepsilon_{\text{diatom}}^{30}$  derived for the *Stephanodiscus* dominated Yellowstone Lake (Zahajská et al., 2023) – also hydrothermally influenced – seemed to be closer to the canonical  $-1.1\text{‰}$  value of (De La Rocha et al., 1997a). Other environmental factors may also play a role but are not yet fully understood (Alleman et al., 2005; Panizzo et al., 2017; Sun et al., 2013, 2018).

Ultimately, the question of whether diatom Si isotope fractionation is intrinsically different between species (or even strains), or whether the observed differences reflect poorly understood environmental controls remains to be adequately answered. What is clear is that  $-1.1\text{‰}$  (De La Rocha et al., 1997a) remains a remarkably good approximation of average  $\varepsilon_{\text{diatom}}^{30}$  (Fig. 4), although we cannot assume that  $\varepsilon_{\text{diatom}}^{30}$  is

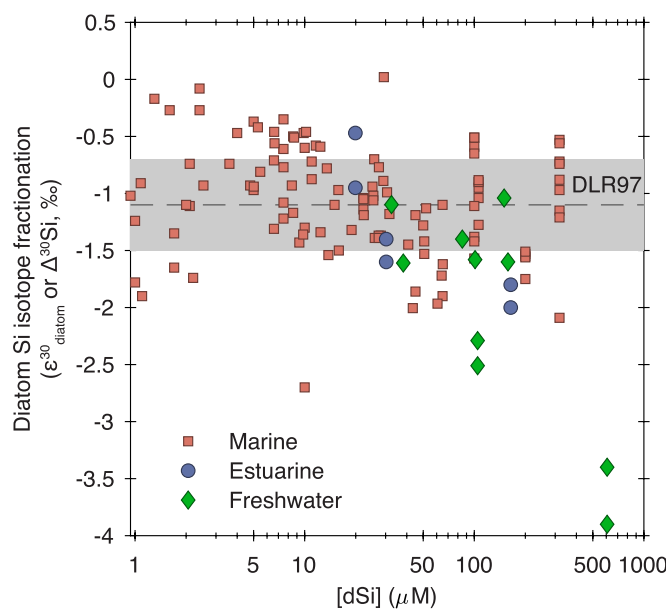


**Fig. 4.** Compilation of published estimates of Si isotope fractionation associated with diatom silicification across freshwater, estuarine and marine environments, plotted as a function of dSi concentrations. Fractionation estimates include those derived from both experiments and interpretations of field data using either a steady-state model (Eqns (1) and (2)) or a Rayleigh model (Eqns. (3) and (4)), resulting in an estimate of  $\varepsilon_{\text{diatom}}^{30}$ . Where deriving the term  $f_{\text{Si}}$  is not possible, fractionation estimates are simply an isotope difference (i.e.  $\Delta^{30}\text{Si}$ , see Box 1) between diatom  $\delta^{30}\text{Si}$  and dSi  $\delta^{30}\text{Si}$ . Dashed line and grey shading show the canonical estimate of  $-1.1 \pm 0.4\text{‰}$  from (De La Rocha et al., 1997a) for cultures of three marine taxa. Data (converted from  $\delta^{29}\text{Si}$  to  $\delta^{30}\text{Si}$  where appropriate) are from: (Alleman et al., 2005; Annett et al., 2017; Beucher et al., 2008, 2011; Cao et al., 2012, 2015; Cassarino et al., 2017; Cavagna et al., 2011; Closset et al., 2015, 2019; Coffineau et al., 2014; De La Rocha et al., 1997a; Doering et al., 2016; Egan et al., 2012; Ehler et al., 2012; Fripijat et al., 2007, 2011a, 2012; Grasse et al., 2021b; Meyerink et al., 2017, 2019; Milligan et al., 2004; Opgelelt et al., 2011; Panizzo et al., 2017; Reynolds et al., 2006; Schmidtbauer et al., 2022; Sun et al., 2013, 2014, 2018; Sutton et al., 2013; Varela et al., 2004, 2016; Weiss et al., 2015; Zhang et al., 2015, 2020).

invariant. Indeed, many studies have demonstrated that diatom Si isotope fractionation varies between species (Fig. 4), implying the need to evaluate the species composition of the studied samples (Beucher et al., 2008; Closset et al., 2015; De La Rocha et al., 1998; Egan et al., 2012; Ehler et al., 2012; Etourneau et al., 2012; Schmidtbauer et al., 2022; Sutton et al., 2013; Varela et al., 2004). Complicating matters is the observation that diatom assemblage composition in sediments does not necessarily represent the abundance nor species composition present in the water column in the past due to potential taxa-specific preservation biases (Pike et al., 2008; see also Section 4). Interpretation of diatom  $\delta^{30}\text{Si}$  variability in terms of past conditions should be undertaken cautiously, particularly when comparing records between geographically distinct sites given that the environmental context and  $\delta^{30}\text{Si}$  of source waters (preformed and regenerated) has a governing role in the  $\delta^{30}\text{Si}$  of diatoms.

#### 4. The influence of diagenesis on the preserved Si isotope signal

Using diatoms as an archive depends on their availability in sediments, and that their geochemical composition is unchanged. (Sea) water is generally undersaturated with respect to bSi (e.g. Hurd, 1973) with the implication being that diatom bSi should progressively dissolve in the water column before reaching the bottom. Yet we still observe diatom bSi in sediments, implying the dissolution is incomplete. For example, Jansen and van der Gaast (1988) found a downcore decrease in

bSi of only 5% in 100,000 years. At face value, this creates a conundrum leading to the conclusion that multiple processes must influence the dissolution/preservation behaviour of diatom bSi. One or more can act simultaneously, affecting not only the preservation of bSi in general, but potentially also the Si isotope composition of the preserved diatoms. In the following, we first outline how and why the dissolution process does not treat all diatom bSi equally, and then explore the implications for the preservation of a  $\delta^{30}\text{Si}$  value during burial and diagenesis.

#### 4.1. Biogenic opal dissolution processes

Diatom bSi consists of a random packing of  $[\text{SiO}_4]$ -units. Silica particles carry a surface negative charge that will interact with the biogeochemical environment. The tetrahedrally bonded  $>\text{Si}-\text{O}-\text{Si}<$  (siloxane) is surrounded by a less dense hydrous layer consisting of  $-\text{Si}-\text{OH}$  groups (silanols) (Gendron-Badou et al., 2003). Dissolution of silica in aqueous solutions is mainly due to hydrolysis and breaking of the  $>\text{Si}-\text{O}-\text{Si}<$  bonds (Dove and Crerar, 1990; Loucaides et al., 2010a; Sjöberg, 1996). The dissolution rate is therefore variable (Fig. 5) and depends on the structure of the bSi and degree of disequilibrium between the solid silica and the surrounding solution. At 25 °C and 1 bar, reported solubilities of diatom silica in seawater vary anywhere from 200 to  $>1600\text{ }\mu\text{M}$  (Fig. 5; Hurd, 1972; Loucaides et al., 2012a; Loucaides et al., 2012b; Loucaides et al., 2008; Van Bennekom et al., 1991; Van Beueskom et al., 1997). The highest values generally correspond to fresh diatom frustules grown in open ocean seawater. Dissolution is not necessarily homogeneously distributed over the diatom bSi, but rather localized and centered on surface defects, e.g. small pores or compositional defects (Van Cappellen and Qiu, 1997a).

Solubility of diatom bSi increases with increasing temperature, whereby a typical temperature gradient between the ocean surface and the deep-sea of  $\sim 20\text{ }^{\circ}\text{C}$  leads to a decrease in solubility by nearly 50% (Hurd, 1972, 1973; Kamatani, 1982; Lewin, 1961). Pressure changes, on the other hand, have only a relatively minor influence on solubility (Loucaides et al., 2012b). Changes in salinity and pH, for example during the freshwater-seawater transition in near-coastal environments, strongly influence bSi solubility and dissolution rate constants. Increasing pH in seawater leads to the deprotonation and breaking of the silica surface  $-\text{Si}-\text{OH}$  groups, which may be promoted by adsorbed alkali cations like  $\text{Na}^+$  and  $\text{Mg}^{2+}$  increasing solubility and dissolution rates (Dove, 1994; Dove and Elston, 1992). Other adsorbed cations like  $\text{Al}^{3+}$  work in the opposite direction reducing solubility and dissolution rates (see also below; Ille, 1979).

Diatom bSi formation is highly dynamic, with certain frustule parts being formed after each other (Hildebrand et al., 2018 and references therein). Si content and the degree of interconnections between  $\text{SiO}_4$  units thereby varies both between species and within specimens. Tesson et al. (2009) identified two types of Si at diatom surfaces: in *Thalassiosira pseudonana* the majority of Si was associated with the condensed silica, whereas in *Phaeodactylum tricornutum* Si was predominantly found in a weakly polymerized form. In addition, environmental growth conditions, including nutrient and trace element availability, influence the degree of silicification of the frustule (as well as its Si isotope fractionation; see Section 3) (Baines et al., 2010; Leynaert et al., 2004, 2018; Marchetti and Cassar, 2009; Martin-Jezequel et al., 2000; Meyerink et al., 2017). Accordingly, diatom bSi solubility varies between different species and different parts of diatoms (Fig. 5b). This means dissolution of bSi frustules can be a multistep process when the frustule consists of different biomimetic phases with differing dissolution behaviour due to e.g. different chemical properties or because they are associated to more or less refractory pools of organic material (Boutorh et al., 2016; Gallinari et al., 2002; Moriceau et al., 2009). In general, frustule or parts of frustules with high specific surface area or delicate structures of the bSi skeletons dissolve faster, which leads to the loss of surface area during sinking and burial (Fig. 5c) and the preferential sediment burial of more heavily silicified diatom species or parts of diatom frustules (Battarbee

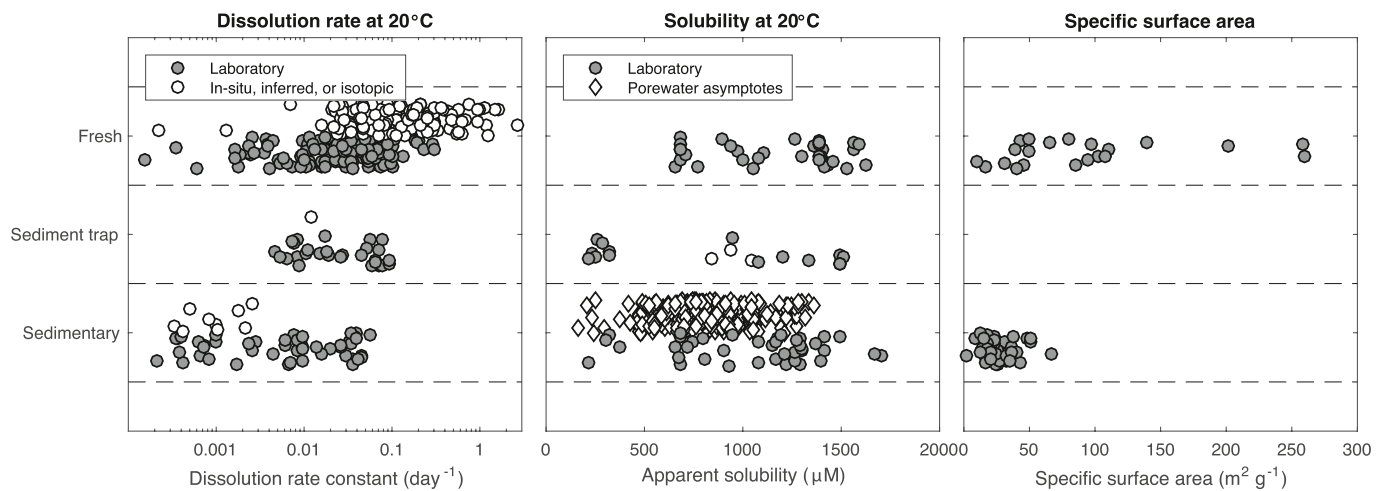


**Fig. 5.** Compilation of published dissolution rate constants ( $\text{day}^{-1}$ ; panel A) and apparent solubilities ( $\mu\text{M}$ ; panel B) and specific surface area ( $\text{m}^2 \text{ g}^{-1}$ ; panel C) for 'fresh', sediment-trap, and 'sedimentary' material. Fresh material includes e.g. plankton tows and diatom cultures, while sedimentary material includes samples ranging from modern core tops to pre-Quaternary. Data from *in-situ* field experiments are presented as open symbols, and laboratory determinations as closed symbols. Most, though not all, experiments were carried out in 0.7 M NaCl amended with Tris solution, and not all were carried out at 100% undersaturation. Estimates of bSi solubility from asymptote values of dissolved Si concentrations in panel B are from (Frings, 2017). In (A), all the data have been rescaled to a common temperature of 20 °C assuming the temperature dependence can be expressed as an Arrhenius law with an activation energy of 60 kJ mol<sup>-1</sup> (see Rickert et al. (2002) for details). In (B), all data have also been rescaled to 20 °C using eqn. (11) of Rickert et al. (2002) that captures the gradient of temperature-solubility relationship empirically determined elsewhere. The *in-situ* temperature for the porewater asymptote data is taken from the WOCE global hydrographic climatology Gouretski and Koltermann (2004). Only data representing chemically untreated material (i.e. not acid or H<sub>2</sub>O<sub>2</sub> washed) is included in this compilation. Data from: Van Cappellen et al. (2002), Cheng et al. (2009), Rickert et al. (2002), Nelson et al. (1976), Kamatani (1982), Tréguer et al. (1989), Wu et al. (2015), Gallinari et al. (2002), Van Cappellen and Qiu (1997a, 1997b), Bidle et al. (2003), Ehrenhauss et al. (2004), Nelson and Gordon (1982) and Nelson and Goering (1977).

et al., 2005; Dixit et al., 2001; Hurd, 1973; Van Cappellen and Qiu, 1997a).

In living diatom cells, the bSi skeleton is protected from dissolution through an outer organic layer, which is disrupted as soon as they die (Bidle and Azam, 1999; Hecky et al., 1973; Lewin, 1961). The dissolution rate of diatom frustules free from organic coatings is directly proportional to the surface area of the interface between the bSi and the surrounding water (Loucaides et al., 2012a). Afterwards, metal ions from natural water like Mg, Fe, and Al adsorb to the bSi surface, forming coatings (see also below) to reduce either dissolution rate and/or the solubility (Lewin, 1961). Al is one of the most effective elements in combining with bSi because the hydrated Al<sup>3+</sup> cation reacts with the hydroxyl groups at the bSi surface, therefore decreasing dissolution (Hurd, 1973; Iler, 1979). Both organic and cation layers determine the diffusion of dSi to and from the interface between the dissolving bSi skeletons and the solution, and therefore control the dissolution rate (Kamatani et al., 1988).

#### 4.2. Modification of the Si isotope signal during (partial) dissolution

As mentioned above in Section 3, Si isotope fractionation by diatoms is not constant but instead reflects multiple factors that likely include external (micro)nutrient availability and internal cellular processes such that the frustule archives may record information in addition to dSi utilization (Cassarino et al., 2021). Although this process is not yet understood in detail, it might have significant effects on the preservation of a "pristine" surface water Si isotope signal in diatoms: if Si isotope fractionation differs during uptake and precipitation, then variable timing of precipitation of different parts of the frustule, and subsequent partial dissolution of the frustule, might influence the reconstructed Si isotope composition of the remaining frustule parts.

Demarest et al. (2009) investigated the dissolution of fresh diatom bSi in the laboratory (corresponding to water column processes) and reported Si isotope fractionation, whereby lighter isotopes were preferentially released with an enrichment factor  $\epsilon_{\text{DSi-BSi}}^{30}$  of  $-0.55\text{\textperthousand}$ , which was independent of species or temperature. A similar finding was

reported by Sun et al. (2014) for natural samples from the Baltic Sea. In contrast, other laboratory (Wetzel et al., 2014) and field studies (Closset et al., 2022; Panizzo et al., 2016) did not find any evidence of resolvable Si isotope fractionation during bSi dissolution. However, Sun et al. (2014) also stated that the isotope effect was just observed in the solution and not the residual bSi fraction. Similarly, Demarest et al. (2009) noted that the effect could only be observed at certain dissolution rates and that the inferred maximum possible change in  $\delta^{30}\text{Si}_{\text{diatom}}$  of  $+0.55\text{\textperthousand}$  would likely not be significant in natural sediments due to high mean percentage of dissolution including complete loss of the more soluble members of the diatom assemblage. Similarly, Wetzel et al. (2014) calculated that at least 25% partial dissolution would be required to produce an isotope shift outside the typical measurement uncertainties. This implies that the observed fractionation during dissolution in the studies of Demarest et al. (2009) and Sun et al. (2014) most likely is an apparent fractionation reflecting e.g. the partial loss of isotopically light diatoms from the community rather than the actual release of the lighter isotopes from the bulk bSi. This means in nature, with largely complete dissolution of less silicified diatom material and complete preservation of the most robust, generally well-preserved frustules, fractionation during dissolution does not play a significant role, and the Si isotope composition of diatom bSi appears to be robust against dissolution in the deep-sea sedimentary environment (Wetzel et al., 2014).

In addition to the experimental and empirical evidence that suggests [true] fractionation during dissolution does not introduce bias to diatom  $\delta^{30}\text{Si}$  records, there are also strong theoretical arguments as to why this should be the case. Paradoxically, this starts by acknowledging that as a process that involves the net transfer of Si from one phase (bSi) to another (dSi), there will almost certainly be an isotope effect, whether kinetic or equilibrium (Box 1). However, this argument also acknowledges that dissolution is by definition a surface process that proceeds inwards. The implication is that during the very first stages of dissolution, any isotope fractionation that results in the preferential transfer of the lighter isotopes to the dissolved phase will, by mass balance, require that a surface layer remains that is enriched in the heavier isotopes. Therefore, over the timescales it takes for the surface layer to develop

and progress inwards, the net effect is the congruent (i.e. complete) dissolution of the frustule. This is most clearly seen in the mineral dissolution literature for a range of isotope systems, including Si (Ziegler et al., 2005), but also Fe (Kiczka et al., 2010), Mg (Pokharel et al., 2019) and Zn (Weiss et al., 2014), among others. If the same is true for diatom bSi, it is only the early stages of dissolution that will induce a fractionation. Importantly, this will very likely be unresolvable in the bulk remaining solid.

Further arguing against dissolution substantially biasing the preserved bSi  $\delta^{30}\text{Si}$  record are multiple core top and sediment trap studies that show that the diatom Si isotope composition faithfully record the  $\delta^{30}\text{Si}$  of exported bSi, both in seawater and freshwater environments (Egan et al., 2012; Ehlert et al., 2012; Grasse et al., 2021a; Panizzo et al., 2016). If dissolution were to play a significant role, then this should not be the case in such vastly different environments with variable bSi content and preservation.

In summary, partial dissolution of diatom bSi in the water column and in sediments leads to preferential loss of less silicified frustule structures – at the scale of individual frustules, but also at the assemblage scale. This can, under certain circumstances, lead to an apparent Si isotope fractionation with the remaining bSi appearing isotopically distinct relative to the initial bSi. The available empirical studies so far indicate that this process is largely negligible in natural systems. However, during the extraction of the bSi from the sediments, monitoring the condition of the bSi is advisable, and samples with diatom frustules with poor preservation should be avoided or at least interpreted carefully (see also Section 6).

#### 4.3. Exchange processes between biogenic opal and the environment

In addition to protecting surface layers on the outside of the diatom bSi, exchange reactions with other components from seawater and/or sediment strongly influence dissolution/preservation rates. Over the years multiple studies have shown that trace elements, especially Al, can replace Si in the bSi (Liu et al., 2024). They are incorporated structurally and distributed homogeneously into the silica skeleton during production both from seawater (Dixit et al., 2001; Gehlen and Van Raaphorst, 2002; Iler, 1979; Liu et al., 2024; Tian et al., 2022; Van Bennekom et al., 1991; van Bennekom et al., 1989) and freshwater (Liu et al., 2019), whereby the amount of trace elements in the bSi correlates with the amount of trace elements in the growth medium (Van Bennekom et al., 1991; van Bennekom et al., 1989). Naturally occurring variations of Al/Si ratios in water, and therefore in the diatom bSi, consequently have a marked influence on the recycling of bSi in different regions. In the water column, dSi and Al are taken up by the diatoms during primary production. During dissolution, however, the Si is removed, whereas the Al is retained, leading to an increase in the Al/Si-ratio in the diatom silica during sinking, deposition and burial in the sediments (Bishop and Biscaye, 1982; Rickert et al., 2002), favouring preservation of the bSi. Interestingly, availability of other trace elements like Fe during primary production influences the Al uptake, with increasing Fe concentrations leading to decreasing Al uptake, which might result in higher solubility of the diatom bSi (see also Section 3) (e.g. Tian et al., 2023).

In sediments, the dissolution kinetics of bSi is assumed to be quite different from seawater because of interactions with coexisting clay minerals and silicates (Kamatani et al., 1988). Generally, deposited bSi will undergo dissolution during its progressive burial, driven by thermodynamic instability, which is reflected by an asymptotic increase in pore water dSi concentrations. However, pore water dSi concentrations vary considerably between regions (Fig. 5b) (Frings, 2017; McManus et al., 1995; Rabouille et al., 1997) and maximum concentrations are often much lower than the expected solubility of pure biogenic/amorphous silica, or even crystalline silica phases (Rimstidt and Barnes, 1980). bSi solubility and dissolution rates decrease significantly with depth due to a progressive reduction of the defect density of the bSi surfaces, through dissolution and reprecipitation of Si (Van Cappellen

and Qiu, 1997a, 1997b).

At the sediment-water interface, detrital minerals dissolve leading to increased Al concentrations in the pore waters. The Al content of the deposited bSi increases with increasing time of exposure, whereby initial Al uptake is rapid (days to weeks) (Koning et al., 2007; Loucaides et al., 2010b). This Al incorporation is associated with structural changes towards e.g. smaller pores, and textural changes consistent with the formation of authigenic Al-silicate phases on e.g. the surface of the diatom bSi and reduction in bSi solubility (Koning et al., 2007; Mackin and Aller, 1984). Both laboratory experiments (Charlet and Manceau, 1994) and natural samples (Van Cappellen and Qiu, 1997a, 1997b) indicate that a continuum exists from unaltered bSi, to partially dissolved bSi, to bSi with adsorbed cations on the surface, to incorporation of cations into the bSi structure, to the formation of surface precipitates with true authigenic clay mineral structure and composition (Loucaides et al., 2010b; Michalopoulos and Aller, 1995, 2004; Michalopoulos et al., 2000).

The key factors driving sedimentary early diagenesis of bSi seem to be the ratio between detrital material and bSi in the sediment, and the type of detrital material (Presti and Michalopoulos, 2008; van Bennekom et al., 1989; Van Cappellen and Qiu, 1997a). In detrital-poor sediments, the bSi solubility is dominantly influenced by structural incorporation of Al into the bSi structure (Dixit et al., 2001). With increasing detrital content, however, solubility and dissolution kinetics of the detrital minerals exert control over the solubility of the bSi (Dixit et al., 2001; Gallinari et al., 2002; Van Cappellen and Qiu, 1997a). Therefore, in sediments with detrital clay minerals with high Al content and dissolution rates, like kaolinite or gibbsite, preservation of bSi is better than in sediments characterized by Al-poor clay minerals like smectites, illite or chlorite (Griffin et al., 1968; Johnson, 1976; van Bennekom et al., 1989; Wollast, 1974).

#### 4.4. Modification of the Si isotope signal during exchange processes

The supply of dSi to pore waters from dissolving bSi is typically counterbalanced by the removal of dSi via precipitation of authigenic silicate phases, even in significantly undersaturated conditions, suggesting that adsorption is an integral part of the dissolution reaction (Fig. 6) (Truesdale et al., 2005). Indeed, field investigations using Si isotopes indicate a dynamic balance between the dissolution of bSi or reactive lithogenic silica phases, and silica re-precipitation, where the relative importance of each process differs significantly between regions. Simultaneous bSi dissolution and formation of authigenic silica has been observed in e.g. tropical deltas (Pickering et al., 2020; Rahman et al., 2017), in glacially-influenced coastal regions (Ng et al., 2020, 2022) as well as in open ocean shallow shelf areas to deep hadal trench settings (Closset et al., 2022; Ehlert et al., 2016; Geilert et al., 2020, 2023; Huang et al., 2023; Luo et al., 2022; Ward et al., 2022a, 2022b). Although the exact compositions of the authigenic precipitates are often unknown, they are suggested to be enriched in the lighter Si isotopes compared to the source. Estimated Si isotope fractionations  $\epsilon_{\text{authigenesis}}^{30}$  generally range between  $-2\text{\textperthousand}$  and  $-3\text{\textperthousand}$  (Ehlert et al., 2016; Geilert et al., 2023; Pickering et al., 2020; Ward et al., 2022a, 2022b). In natural settings, those fractionations probably reflect a net effect of multiple processes and authigenic phases, depending on the sediment and pore water composition. The values are, however, in general agreement with laboratory and modeling studies.

The magnitude of the kinetic isotope effect for Si isotopes during laboratory precipitation of pure amorphous silica from a (over-)saturated dSi solution has been shown to vary with temperature and precipitation rate, ranging between  $\Delta^{30}\text{Si}_{\text{solid-fluid}}$  of  $-3.5\text{\textperthousand}$  (Roerdink et al., 2015) or  $-2.1\text{\textperthousand}$  at  $10^\circ\text{C}$  (Geilert et al., 2014) and  $-0.4\text{\textperthousand}$  to  $-1\text{\textperthousand}$  at room temperature (Li et al., 1995). During precipitation with and without addition of dissolved Al, pure amorphous silica without Al shows no Si isotope fractionation, whereas in high-Al conditions the silica precipitate is up to  $5\text{\textperthousand}$  lower  $\delta^{30}\text{Si}$  than the source (Oelze et al.,

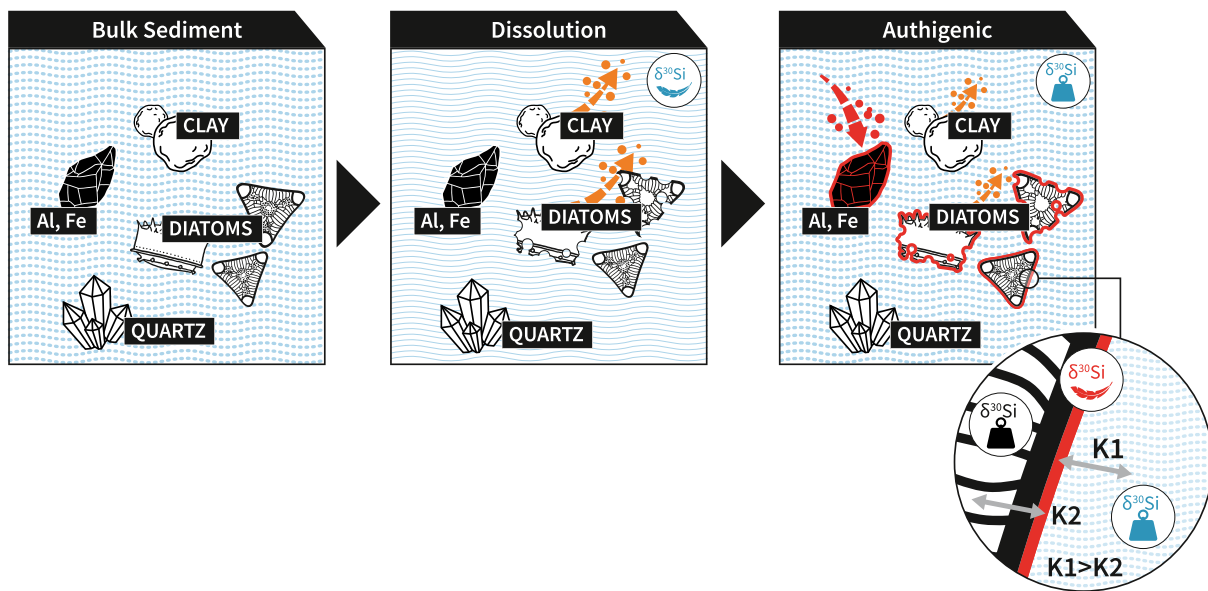


**Fig. 6.** Schematic of processes occurring during bSi diagenesis in sediments and their influence on the preserved diatom Si isotope composition. a) Typical bulk sediment containing a mixture of e.g. bSi (diatom frustules), silicate minerals (e.g., quartz, feldspars), pedogenic clays and various metal (e.g. Al, Fe) (oxyhydr) oxides. b) Dissolution of any of those phases leads to increase in dSi and other elements, and a decrease in dSi  $\delta^{30}\text{Si}$  in the pore water with no isotope fractionation associated to the dissolution process (Section 4.2). Porewater becomes isotopically lower  $\delta^{30}\text{Si}$  because the dissolving sediment components are typically isotopically lighter than the original pore water (see Section 4.2 for details). c) Due to increased dissolved element concentrations, adsorption/precipitation of secondary amorphous silica and authigenic clay phases binds dSi and other elements like Al and Fe in solid phases. This is dominated by kinetic isotope fractionation and tends to lead to an enrichment of lighter isotopes in the secondary phases (i.e. lower  $\delta^{30}\text{Si}$ , see Section 4.4 for details). The insert d) highlights structural Si isotope exchange (dominated by equilibrium isotope fractionation) between (i) dSi and diatom surfaces and (ii) between surface and interior diatom frustule. Zheng et al. (2019) e.g. showed enrichment of lighter isotopes in the diatom surface compared to the surrounding water (faster exchange rate  $K_1$ ) but enrichment of heavier isotopes within the interior compared to the surface (slower exchange rate  $K_2$ ) (see Section 4.4 for details).

2015b). Similarly, adsorption of dSi onto solid Al hydroxides, precursor phases of clay minerals, produces Si isotope enrichment between  $-1.8\text{\textperthousand}$  to  $-3\text{\textperthousand}$ , with higher fractionation with increasing initial dSi concentration and higher adsorption rates (Oelze et al., 2014). Adsorption of dSi onto Fe oxides produces Si isotope enrichment between  $-0.54$  and  $-0.81\text{\textperthousand}$  (Delstanche et al., 2009; Opfergelt et al., 2009). Actual clay separates with a predominant smectite composition were found to be  $0.4\text{\textperthousand}$  lower  $\delta^{30}\text{Si}$  compared to their feldspar source (Georg et al., 2009a, 2009b), and larger magnitude fractionations (as large as  $-3.4\text{\textperthousand}$ ) are observed for clays with kaolinite-like composition (Frings et al., 2021). This implies that the chemical composition and pathway of formation of the precipitating silicate should have a strong influence on the Si isotope fractionation. An apparent Si isotope enrichment of  $-2\text{\textperthousand}$  to  $-3\text{\textperthousand}$  – typically inferred from an inversion of pore water  $\delta^{30}\text{Si}_{\text{dSi}}$  profiles (Ehlert et al., 2016) – in natural sediments is consistent with the formation of multiple authigenic Si-containing phases during early diagenesis in sediments. Using sequential acidic and alkaline leaching, Pickering et al. (2020) indeed identified isotopically distinct pools: metal-Si hydroxides with a very light Si isotope composition, as well as authigenically altered and unaltered bSi with heavier Si isotope compositions. Interestingly, dissolution of bSi followed by re-precipitation of Al-silicates (often termed “altered bSi” in the literature, mostly equivalent to authigenic Al-silicate phases) should lead to the altered fraction being isotopically lighter than the bSi source itself if the kinetic isotope effects discussed above dominate. Pickering et al. (2020), however, calculated that the Si isotope composition of the authigenic silicate fraction was, on average,  $0.56\text{\textperthousand}$  heavier than the bSi. This is corroborated by a recent inverse modelling study assuming isotopic mass balance between marine Si sources and sinks, which shows that the global average Si isotope composition of authigenic Al-silicate phases in marine sediments ( $+1.31 \pm 2.96\text{\textperthousand}$ ) is slightly higher but does not differ strongly from global average bSi of diatoms ( $+1.00 \pm 0.74\text{\textperthousand}$ ) (Rahman and Trower, 2023). The estimated distribution of the Si isotope

composition of authigenic phases, however, encompasses a greater range than that of diatoms (Rahman and Trower, 2023). This probably reflects differences in the sediment geochemical composition and consequently variety of authigenic phases that can form.

Adsorption of dSi and/or precipitation of authigenic Al-silicates is dominated by unidirectional kinetic isotope fractionation (Dupuis et al., 2015; Oelze et al., 2015a). The subsequent dissolution/precipitation reactions and interaction between bSi and other sedimentary solid and liquid phases gradually shift the composition towards a steady-state characterized more by equilibrium isotope fractionation (Box 1) (Fernandez et al., 2019; Oelze et al., 2014). In principle, this is a mechanism to modify the  $\delta^{30}\text{Si}$  of bSi without any obvious structural or geochemical fingerprint through isotope exchange reactions between the bSi, pore water dSi and/or precipitated authigenic Si. Isotope exchange/equilibrium isotope fractionation is generally slower than kinetic isotope fractionation. However, Oelze et al. (2014) showed adjusted isotope equilibrium between dSi and Si adsorbed onto amorphous Al hydroxides is attained within approximately two months. Similarly, experiments between Fe-Si gel and solution (Zheng et al., 2016) and between amorphous silica and solution (Zheng et al., 2019) showed up to 90% Si isotope exchange within less than 126 days. The magnitude of isotope fractionation during exchange is still under investigation. Oelze et al. (2014) reported an enrichment factor close to  $0\text{\textperthousand}$ , although it is unclear whether their experimental design actually reflected equilibrium fractionation conditions. Stamm et al. (2019) found that isotope exchange between amorphous silica and solution is temperature- and pH-dependent. At pH 6 and  $25^\circ\text{C}$  the equilibrium isotope fractionation was  $0.45 \pm 0.2\text{\textperthousand}$  with the lighter isotopes enriched in the fluid, whereas at pH  $> 9$  the fractionation was  $1.63 \pm 0.23\text{\textperthousand}$ . Isotope enrichment decreased with increasing temperature (Stamm et al., 2019). To complicate matters, there is likely multiple Si isotope exchange processes that occur with different exchange rates and fractionation factors (Zheng et al., 2016, 2019) (Fig. 6d). A dominant,

faster exchange is associated with surface sites with a best estimate of equilibrium Si isotope enrichment between bulk amorphous solid silica and aqueous dSi in seawater at pH 7.3, 23 °C of  $-0.52\text{\textperthousand}$  (Zheng et al., 2019). Slower exchange occurs between exterior and interior Si atoms of the solid, with no fractionation factor estimated (Zheng et al., 2019). In other words, exchange with surface sites tends to partition the heavier Si isotopes in the aqueous phase relative to the solid surface, counter to the findings of Stamm et al. (2019), whereas exchange between surface and interior sites in the solid tends to enrich heavy Si isotopes in the interior (Fig. 6d) (Zheng et al., 2019). Thereby, higher surface area of the solid corresponded to faster and more extensive Si isotope exchange (Fernandez et al., 2019), which is enhanced by higher ionic-strength in the solution because it promotes the breakage and formation of new -Si-O bonds (Fernandez et al., 2019; Zheng et al., 2019). This would indicate that equilibrium isotope fractionation could alter the preserved Si isotope composition of diatoms in sediments through exchange between bSi, pore water dSi and/or surface precipitates of authigenic silicates. Here, the isotope composition of the authigenic precipitate (e.g. very light Si isotope composition of metal (hydr)oxides or a more diatom-like composition of Al-silicate phases, see above) may affect the extent of isotope exchange as well as the  $\delta^{30}\text{Si}$  of the porewater dSi. However, low surface areas, which are attained quickly within sediments, seem to protect or preserve solid phase isotopic signatures (Fernandez et al., 2019). The extent and direction of this Si isotope alteration, however, still warrant further investigation.

Diatom bSi-bound  $\delta^{18}\text{O}$  provide additional insight into possible exchange reactions and their impact on the preserved isotope signal in the sedimentary record. Oxygen in bSi is also found in the two main types of bonds: >Si–O–Si< and -Si–OH. The -Si–OH bonds are less stable and may experience oxygen isotope exchange (Leclerc and Labeyrie, 1987) whereas > Si–O–Si < bonds, once formed, are unlikely to undergo isotopic exchange until a phase change occurs (Murata et al., 1977), which is relevant for both oxygen and Si isotopes (see also Section 4.5). Indeed, for  $\delta^{18}\text{O}$ , most significant changes were observed with an initial dehydroxylation/reduction in the structural OH- abundance in the bSi (Dodd et al., 2017; Menicucci et al., 2017). Incubation experiments with  $^{18}\text{O}$ -enriched seawater, representing conditions during sinking through the water column and initial deposition at the sediment-water interface, show that significant  $^{18}\text{O}$ -exchange at both external and internal groups occurs throughout diatom frustules for both fresh and fossil specimens over very short timescales (of days to weeks) (Akse et al., 2020). Although conventional sample handling protocols for analysing bSi-bound  $\delta^{18}\text{O}$  involve, for example, a step-wise fluorination to remove altered surface OH-bonded  $^{18}\text{O}$ , post-mortem changes in  $\delta^{18}\text{O}$  are still observed (Dodd et al., 2017; Tyler et al., 2017). This indicates that the final measured  $\delta^{18}\text{O}$  in bSi most likely represents a mixture of signals from the original growing stage, water-column settling, and sediment pore waters, and the  $\delta^{18}\text{O}$  signal may be dominated by early diagenetic conditions (Akse et al., 2020; Dodd et al., 2017). In addition, the availability of Al influences  $\delta^{18}\text{O}$  exchange, whereby increasing structural incorporation of Al into the bSi leads to a significant decrease in oxygen isotope exchange (Akse et al., 2022). A similar behaviour may be expected for Si isotope exchange, although to the best of our knowledge no study has yet presented robust proof. While Al present as surface contaminants (clays or other Al-silicates) had no such inhibitory role on the oxygen isotope exchange (Akse et al., 2022), the formation of Al-silicates can, however, result in a negative charge which repels the hydroxyl ions responsible for silica dissolution (Iler, 1979).

In summary, there are multiple processes affecting the preservation of bSi and possibly its Si isotope composition. Dissolution of bSi (with limited associated Si isotope fractionation, see Section 4.2) is typically accompanied by authigenic Si precipitation forming surface layers on sediment particles or replacing the bSi over time completely. Precipitation of Si with metal (hydr)oxides produces new solids with a very low  $\delta^{30}\text{Si}$ , whereas Al-silicate precipitates tend to have an  $\delta^{30}\text{Si}$  similar to that of the bSi. In both cases, the occurrence of such authigenic phases

could affect the reconstructed Si isotope composition of the bSi. However, the techniques commonly used to separate bSi from sediments for Si isotope ratio determination should remove metal (hydr)oxides via e.g. acid leaching (see Section 6 below). This also applies for Al-silicates, although probably to a lesser extent as the removal of those phases is more complicated. Consequently, the direct influence of authigenic precipitates on the preserved Si isotope composition of bSi is expected to be small.

The actual extent of isotope exchange between bSi, (pore) water dSi and any precipitate layer, and its potential effects on the  $\delta^{30}\text{Si}$  of the preserved bSi, is much less clear. In the water column, equilibrium Si isotope exchange reaction rates are probably rather slow in comparison to sinking of the bSi. In combination with low dSi concentrations in seawater, this implies that the initial Si isotope signals locked in diatoms by upper-ocean processes are resistant to re-equilibration during sinking in the water column. In sediments, although dSi concentrations are much higher, decreasing diatom surface area and increasing Al content may lead to slower or even ceasing Si isotope exchange rates, which should facilitate long-term preservation of the original Si isotope signatures in diatom bSi.

#### 4.5. Longer-term re-crystallisation

Over longer timescales, bSi produced by biosilicifiers undergoes diagenetic alteration to reach the thermodynamically more stable silica polymorph quartz. The pathway of this alteration is well studied (Williams and Crerar, 1985; Williams et al., 1985), and in most cases proceeds as a series of transformations from opal-A via opal-CT (a mix of cristobalite and tridymite) to microcrystalline quartz. Each successive phase is structurally distinct and has a higher degree of crystallinity than the preceding phases, which is classically seen in XRD spectra (Liesegang and Tomaschek, 2020; Pisciotto, 1981), and more recently explored via FTIR and Raman spectroscopy (Stamm et al., submitted). Opal-A is hydrated (ca. 10% H<sub>2</sub>O content) and amorphous while opal-CT comprises a much less-hydrated disordered layering of tetragonal ( $\alpha$ -cristobalite) and orthorhombic ( $\alpha$ -tridymite) polymorphs. Opal-CT is typically found as lepispheres - nm to  $\mu\text{m}$ -scale spherical aggregates. Microcrystalline quartz comprises tetrahedrally coordinated SiO<sub>2</sub> and is the most stable form under seawater or sediment conditions. The relevance for application of bSi-based geochemical proxies is that the transformations are well established to happen by dissolution-reprecipitation mechanisms. The strongest line of evidence for this comes from  $\delta^{18}\text{O}$  in bSi, where stepwise changes are observed both in exposed terrestrial sections (e.g. Monterey Bay formation, California) and also downcore in IODP holes (Ibarra et al., 2022; Yanchilina et al., 2020, 2021). The interpretation is that the oxygen isotopes ratios are reset to values in equilibrium with local pore water, which typically will be at a higher temperature than the overlying seawater due to the geothermal gradient. The higher temperature implies a smaller fractionation (Sharp et al., 2016). For a ‘sediment buffered’ system like Si (i.e. Si in solid phase  $\gg$  dSi in pore fluids, per unit sediment volume) mass-balance dictates that the  $\delta^{30}\text{Si}$  of the sediment as a whole should be retained over some spatial smoothing scale, but the extent of this scale is unclear: it may range from individual microfossils to multiple meters. The implication is that if bSi is recrystallized towards an opal-CT or quartz structure, then interpreting  $\delta^{30}\text{Si}$  values or other geochemical proxies as pristine must be done with extreme caution. In the Quaternary, recrystallized bSi is rare because neither time nor temperature have been sufficient to induce the transformation (Tatzel et al., 2022) – although rare localities are known (Tatzel et al., 2015). For older material, it remains an outstanding challenge to be addressed.

#### 5. Influence of dissolved Si source composition on diatom $\delta^{30}\text{Si}$

A key term in all diatom  $\delta^{30}\text{Si}$  based interpretations of palaeoproductivity is the  $\delta^{30}\text{Si}$  of source dSi (i.e. Eqns (1)–(4)), which in

marine environments is often implicitly taken to be constant. A change in  $\delta^{30}\text{Si}$  of source dSi can fundamentally be accomplished by two mechanisms. The first is by changing  $\delta^{30}\text{Si}$  of the whole system (whether lake or ocean) by changing the magnitude and/or  $\delta^{30}\text{Si}$  of the various input fluxes. The second – less applicable to smaller lakes – is by altering regional circulation, such that a given locality receives dSi from a different source and thus with potentially different  $\delta^{30}\text{Si}$ .

### 5.1. Changing $\delta^{30}\text{Si}$ of dSi at the scale of the whole ocean

An assumption of constant ocean  $\delta^{30}\text{Si}_{\text{dSi}}$  over Quaternary timescales is often justified by invoking the long residence time of dSi in the ocean such that it is insensitive to changing external input flux magnitudes or isotope compositions. This may not be a reasonable assumption for all Quaternary timescale  $\delta^{30}\text{Si}$  applications. Simple frameworks imply that residence time is the key metric determining the timescales over which external forcings must be considered (Mokadem et al., 2015; Richter and Turekian, 1993). In short, the geochemical response to a changing flux will be strongly related to the relative magnitude of the change on timescales equivalent to or greater than the residence time, and attenuated on timescales shorter than this. Recent estimates of residence time for dSi in the ocean cluster around 10 ka (see discussion in Tréguer et al., 2021). Residence times of dSi in lakes are hugely variable, from days to millennia (Frings et al., 2014a). Thus, even for the ocean and large lakes, we cannot neglect the possibility that changing  $\delta^{30}\text{Si}$  and/or changing balance of dSi sources are modifying the whole-system dSi  $\delta^{30}\text{Si}$  over timescales relevant for many Quaternary applications (Frings et al., 2016; Georg et al., 2009a; Opfergelt et al., 2013; Sutton et al., 2018a). The implication is that we should not directly interpret Si isotope records without first deconvolving any whole-system change.

There is reasonably strong evidence for whole-system change in dSi  $\delta^{30}\text{Si}$ . In the oceans, where most work has focused, an indication lies in the apparent synchrony of most published  $\delta^{30}\text{Si}$  records – across groups of biosilicifiers and between ocean basins – from the last glacial maximum towards the Holocene (Frings et al., 2016; see Fig. 2 in Sutton et al., 2018a). This pattern of low glacial  $\delta^{30}\text{Si}$ , higher interglacial  $\delta^{30}\text{Si}$  also repeats itself in other Quaternary glacial cycles (Griffiths et al., 2013; Kim and Khim, 2017). The conventional interpretative framework would see this as evidence for biosiliceous productivity increasing globally during interglacials, which is hard to justify. Given our understanding on the continental Si cycle and the controls on the flux and  $\delta^{30}\text{Si}$  of dSi flux delivered to the ocean, there are also qualitative reasons to expect the input fluxes of dSi to be lower in  $\delta^{30}\text{Si}$  during glacials (Frings et al., 2016; Georg et al., 2009a; Opfergelt et al., 2013; Sutton et al., 2018a). For example, glacial erosion and subglacial weathering is known to provide a source of low- $\delta^{30}\text{Si}$  dSi (Hatton et al., 2019, 2023). Together with a suite of other mechanisms (outlined in Frings et al., 2016), dSi delivered to the ocean could have been substantially lower in  $\delta^{30}\text{Si}$  than present during peak glacial conditions.

A final line of evidence comes from changes in diatom  $\delta^{30}\text{Si}$  during the transition from glacial to Holocene conditions that are strictly too big to attribute to productivity alone. In the common mass-balance frameworks (cf. Eqns. (1)–(4)) the maximum range should be one fractionation, canonically placed at  $-1.1\text{\textperthousand}$  (but see Section 3 and Fig. 4). Yet many records approach or exceed this range. For example, Southern Ocean core RC13-259 (Brzezinski et al., 2002) encompasses diatom  $\delta^{30}\text{Si}$  from  $0.15\text{\textperthousand}$  to  $1.57\text{\textperthousand}$ , implying a physically meaningless change in dSi utilization of  $>100\%$  assuming constant ocean dSi  $\delta^{30}\text{Si}$ . Overall, if the questions addressed by Si isotope geochemistry span longer timescales than lake or ocean residence times, we cannot ignore the possibility for the whole system to be responding to external (i.e. catchment or continental) forcings.

### 5.2. Circulation changes

A second mechanism to change the  $\delta^{30}\text{Si}$  of dSi utilized by diatoms is

via overturning circulation changes. As well as the interbasin pattern in [dSi] shown in Fig. 1b, there is a similar trend in  $\delta^{30}\text{Si}$  (Holzer and Brzezinski, 2015). In broad terms, this pattern emerges from the interaction of surface biogeochemistry (governed preformed dSi), water column dissolution (governing regenerated dSi) and ocean overturning circulation. A change in one or more of these could change the  $\delta^{30}\text{Si}$  and/or [dSi] of upwelling waters elsewhere in the ocean. This might be particularly relevant for sediment cores located near water mass fronts, especially around the Southern Ocean: diatom  $\delta^{30}\text{Si}$  shows latitudinal differences (Cardinal et al., 2007; Closset et al., 2015; Varela et al., 2004), which is likely due to the changes in the  $\delta^{30}\text{Si}$  of the source waters. It may also be that the circulation patterns have remained consistent, but biogeochemistry of the source region has changed, altering the composition and balance between preformed and regenerated dSi in a given water mass (a similar mechanism is part of the original formulation of the silicic acid leakage hypothesis (Matsumoto et al., 2002)). Attributing a change in diatom  $\delta^{30}\text{Si}$  to dSi-utilization rather than overturning circulation is therefore not necessarily straightforward, and requires that consideration is given to other lines of evidence about water mass source and the biogeochemistry of potential source regions. The growing body of work that demonstrates the sponge spicule  $\delta^{30}\text{Si}$ -[dSi] relationship (Fig. 3C) can be interpreted as a water-mass tracer (e.g. Fontorbe et al., 2017; Hendry et al., 2016; Hendry et al., 2012) are particularly promising in this regard.

### 5.3. Specific challenges of palaeoproductionity reconstructions from lacustrine systems

In contrast to most ocean records, lake diatom  $\delta^{30}\text{Si}$  records are more frequently interpreted in terms of catchment processes (Nantke et al., 2021; Street-Perrott et al., 2008; Zahajská et al., 2023) rather than within-lake productivity (Panizzo et al., 2016). The first Quaternary application of  $\delta^{30}\text{Si}$  to lacustrine environments was pioneered for reconstructing catchment biogeochemical cycling over orbital (glacial-interglacial) timescales at Lake Rutundu, Kenya (Street-Perrott et al., 2008). Next, Swann et al. (2010) examined the availability of nutrient supply to lake surface waters over the late Quaternary, as an indicator of catchment weathering. This was followed by Cockerton et al. (2015), reinforcing Street-Perrott et al. (2008) that lower mid-Holocene diatom  $\delta^{30}\text{Si}$  values in East African lakes reflect increased weathering rates and mirrored the regional post glacial vegetation expansion driven by increasing insolation led rainfall. With late Holocene regional aridity occurring after c. 5000 years BP, higher diatom  $\delta^{30}\text{Si}$  values are interpreted as reflecting a lower supply of catchment derived dSi. More recent assessments have also been documented for the Altai region of North Central China, where diatom  $\delta^{30}\text{Si}$  is similarly thought to record a contrasting mid-Holocene climate and therefore supply of dSi to lakes from their catchments (Xiang et al., 2023).

These studies were pivotal in promoting the application of diatom  $\delta^{30}\text{Si}$  as a climate proxy, and in developing understanding of late Quaternary terrestrial biogeochemical cycling. Nevertheless, they were unable to fully disentangle the role of autochthonous (within-lake cycling) and allochthonous (catchment) dSi sources over time: the same dilemma identified above for the marine realm. This question of productivity vs. input forcing motivated the development of modern-day, process-based studies to develop site-specific mechanistic understanding of how catchments and lake processes are recorded in lake sediment. Alleman et al. (2005) paved the way with one of the first assessments of modern day lacustrine  $\delta^{30}\text{Si}$  (as  $\delta^{29}\text{Si}$ ) signatures for Lake Tanganyika and its dominant tributaries. However, this was not accompanied by diatom  $\delta^{30}\text{Si}$ , most likely due to the challenge of sampling sufficient material for Si isotopic analysis. To bridge this gap, sediment trap studies were developed to better underpin within-lake, seasonal biogeochemical cycling (Panizzo et al., 2016) and to reinforce to what degree  $\delta^{30}\text{Si}$  from lake sediment archives can act as a palaeoproductionity indicator (Panizzo et al., 2017) versus a catchment weathering record (Panizzo

et al., 2018b). Currently, the available data is limited in both temporal and spatial coverage. Overall, this body of work reinforces the need to better underpin lacustrine allochthonous and autochthonous drivers of diatom and dSi  $\delta^{30}\text{Si}$  in modern day systems. In turn, it will also be subject to a discussion on species specific fractionation factors, diatom habitat (benthic versus pelagic) and seasonality of blooms (Section 3). Together, this will improve our ability to disentangle the role of wider catchment sources to lakes, nutrient cycling via thermal stratification and wind driven mixing, as well as the role of seasonal nutrient limitation. These investigations will also be site specific, with smaller lakes and catchments responding on much faster timescales compared to lakes with much larger residence times. Where possible, mass balance approaches could be adopted to model Si budgets (Opfergelt et al., 2011; Zahajská et al., 2021).

Overall, the community should continue to advance Si isotope research on freshwater environments, and should especially compare systems of differing catchment sizes and residence times. The role of higher plants (macrophytes) in lake Si cycling is notably under-constrained, but future work could build on a body of literature focusing on wetlands (e.g. Frings et al., 2014b; Struyf and Conley, 2009). The application of systematic sampling and end member analysis for modern-day systems would be worthwhile to better constrain the role of autochthonous and allochthonous forcings on lake Si cycling, and thus improve our capacity to reconstruct past environments. Improved modern-day system characterisation could be used to better constrain *in vivo* diatom species-specific fractionation factors in the lacustrine realm, where there is a conspicuous paucity of data (cf. Fig. 4).

## 6. Practical issues

### 6.1. Biogenic silica cleaning and contamination screening

The focus of studies developing protocols to clean biogenic silica prior to geochemical analyses has been on diatoms, but the issues and approaches are common to all biosilicifiers. The application of diatom assemblage analyses to palaeolimnological and palaeoceanographic studies has a history spanning decades (e.g. Battarbee and Digerfeldt, 1976), with frustule cleaning methodologies initially developed simply to aid species level identification for palaeoecological-based reconstructions. With the advent of geochemical palaeoproxies, in particular isotopic analyses of bSi, diatom frustule cleaning methods became more rigorous to address issues of contamination (e.g. minerals such as occluded clays) that would otherwise bias measurements (relevant here for  $\delta^{30}\text{Si}$ , but also demonstrated for the C, O and N isotope systems). One of the first methodological papers to demonstrate the impacts of clay and silt grain contamination on  $\delta^{18}\text{O}$  signatures and to propose a standardised cleaning protocol, particularly for lake sediments, was Morley et al. (2004). They acknowledged and built on prior sediment cleaning methods (e.g. Juillet-Leclerc, 1986; Leclerc and Labeyrie, 1987; Shemesh et al., 1988) and while this protocol is still widely utilized, it continues to be refined and updated (Swann and Snelling, 2023).

The various published methods for lacustrine and oceanic studies are often adapted to specific sample requirements, but commonalities can be found. Diatom frustule cleaning typically begins with the removal of organic matter, usually with a hydrogen peroxide (30% H<sub>2</sub>O<sub>2</sub>) leach in a water bath (up to 90 °C) which, depending on the organic matter abundance and composition, could last a period of hours to days. This is often preceded or followed by a 5% HCl leach, usually overnight, with the aim of removing carbonates and any adsorbed authigenic precipitates on the surface of diatoms (especially metal (hydr)oxide layers) and also Al-silicates (see Section 4). These steps often prove effective at removing organic and carbonate content from samples, and so form the basis of diatom sample preparation for ecological identification. Others have employed more aggressive oxidative steps, with a short 1:1 nitric acid:perchloric acid leach (Panizzo et al., 2014; Shemesh et al., 1995).

Difficulties can arise due to the presence of clays and other fine minerals which can often become occluded in, share similar properties of, or replace parts of, diatom frustules or other bSi (Fig. 7a; Section 4). It has been found that for Al-bearing trace minerals, they remain stubbornly adhered and are challenging to fully remove (Liu et al., 2024). The chemical leaches above may loosen their adhesion to the frustule so that they are easier to separate via later sieving or heavy liquid separation. Various separation methods have been explored, with heavy liquid density separation (normally sodium polytungstate) the most common approach to isolate frustules (at settling densities between 2.3 and 1.9 g ml<sup>-1</sup>), sometimes after disaggregation in a sodium hexametaphosphate solution. Further challenges arise when samples contain a high proportion of small diatom valves (particularly <20 µm), concomitant with high abundances of silt- or clay-size particles. This is often the case when isolating diatom frustules from lacustrine sediments as freshwater species are often smaller than their marine counterparts, making it harder to remove occluded material. Lacustrine systems are also likely to have a high proportion of detrital lithogenic particles (Fig. 7a). To overcome this, the heavy liquid density separation can involve multiple steps, incrementally reducing the settling density to better target the finer clays and their removal (Panizzo et al., 2016; Swann and Snelling, 2023).

A key step in bSi cleaning and species separation is the adoption of more physical cleaning methods. This includes wet sieving at mesh sizes specific to the range of species frustule sizes present in individual samples. Morley et al. (2004) propose a range beginning at >75 µm, and finishing at 10 µm. Others have tailored this to include a sub-division of 32 µm mesh size, to remove larger non-diatom bSi including sponge spicules and radiolarians (Fig. 7B,C; Panizzo et al., 2014) thereby minimizing contamination of the cleaned diatom bSi to be analysed (see also Sections 3 and 4). In general, sieving should be tailored to the size of the taxa to be targeted. However, breakage of valves can occur via these physical sieving and disaggregation methods including ultrasonication (Studer et al., 2013), which has knock on implications for the subsequent cleaning steps, particularly differential sieving and/or heavy liquid density separation.

Bulk diatom bSi samples for isotopic analysis can be compromised due to inter-species differences in Si isotope fractionation factor, habitat, seasonal growing period and life stage (e.g. resting spores of the marine species *Chaetoceros*) (discussed in Section 3). While various studies have aimed to quantify the possible impacts of these processes on diatom  $\delta^{30}\text{Si}$  values, the full implications are hard to quantify. To circumvent these issues as far as possible,  $\delta^{30}\text{Si}$  records should be generated from mono-specific samples. In rare cases, one species dominates the assemblage (e.g. Zahajská et al., 2023), meaning the cleaning steps outlined above should suffice. Elsewhere, effort must be devoted to separation of individual taxa. Picking of larger taxa (e.g. *Coscinodiscus*, *Ethmodiscus*) as well as most radiolarians and sponge spicules is relatively straightforward with conventional micropaleontological techniques (Doering et al., 2016; Hendry et al., 2014). Snelling et al. (2013) demonstrated the potential to physically extract individual diatom frustules from a bulk sample assemblage via micro-manipulation, building on the earlier work of Stoll and Shimizu (2009). Others have demonstrated that even small taxa can be hand-picked following standard micropaleontological techniques (Nantke et al., 2019, 2021). An advantage of manual selection of is that diatom frustules with a higher proportion of contamination and/or dissolution can also be excluded from the final assemblage, such that the method actively discriminates against contaminant minerals in the sample, acting as a further purification step (Fig. 7d). Micro-manipulation can favour the extraction of centric valves as pennate frustules can rotate sideways and obstruct the capillary tube (Snelling et al., 2013). Both micro-manipulation and hand-picking can be time consuming, depending on the species richness, composition, level of contamination and volume of material needed for analysis. A further option is gravitational split-flow thin fractionation (SPLITT) where laminar flows are used to separate species based on the density of

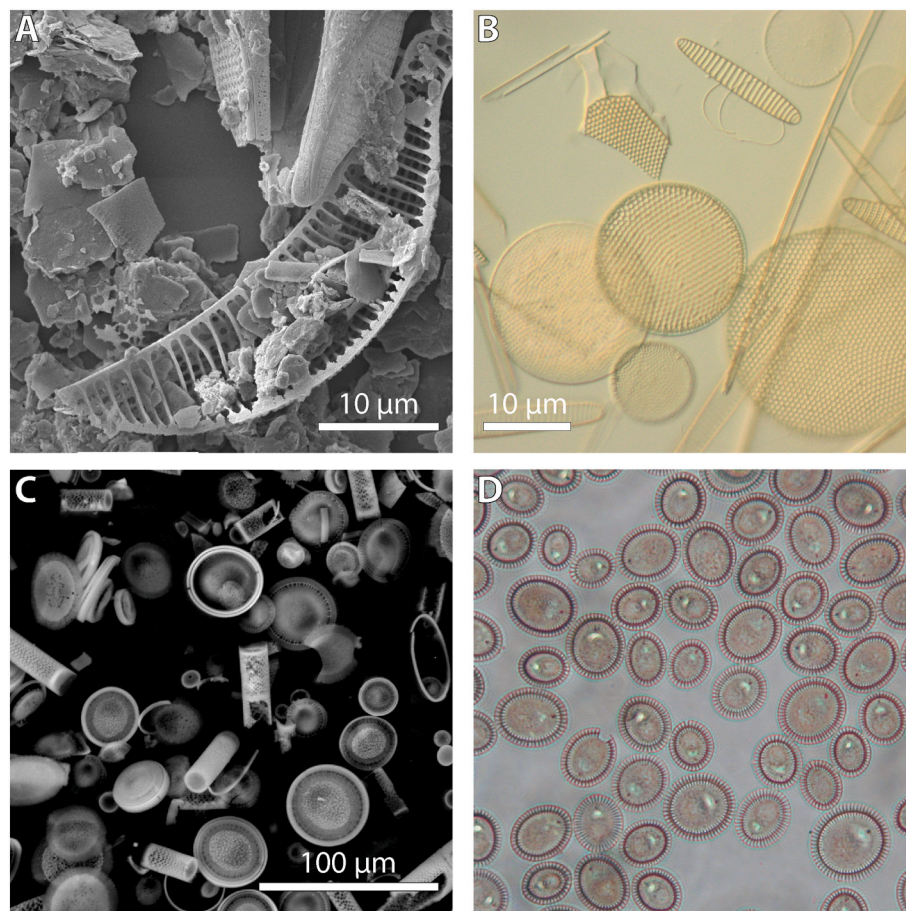


**Fig. 7.** Light Microscopy and Scanning Electron Microscopy images of the different cleaning stages for diatom bSi stable isotope analysis. A: SEM image of freshwater diatom species from Lake Arachlei, south east Siberia, demonstrating how high clay content in samples can compound diatom valve separation and can occlude surface valve punctate, striations and the interior of valves. B: Photomicrograph to demonstrate the effects of wet sieving marine diatom species at >32 µm, as one of the diatom cleaning stages. Sieving at this size means that the larger diatom centric valves are separated from the final diatom composition in an attempt to remove sponge spicules from the final biogenic opal composition. C: SEM image to demonstrate the effectiveness of cleaning stages for freshwater diatom species from Lake Baikal, although also highlighting that diatom valve dissolution could still have taken place and some small chrysophytes may be present. D: example of a near-monospecific final purified sample from Lake El'gygytgyn prepared using the micro-manipulation methods of [Swann and Snelling \(2023\)](#).

individual taxa ([Rings et al., 2004](#)). Wet sieving has sometimes also been applied to try and achieve mono-specific samples (e.g. [Swann et al., 2013](#)). Nevertheless, these cleaning approaches are not guaranteed to yield a mono-specific sample.

Visual inspection via light microscopy and/or SEM of final samples is key to ensure that the diatom composition corresponds to what is desired (e.g. monospecific, as in [Snelling et al. \(2013\)](#), or representative of seasonal assemblage as in [Swann et al. \(2016\)](#) and [Panizzo et al. \(2016\)](#)) and that the abundance of mineralogenic contaminants and other bSi (e.g., sponge spicules, cryophyte cysts) is minimal. Other approaches to characterise the cleanliness of samples ahead of  $\delta^{30}\text{Si}$  analysis involve quantifying the abundance of various elements in the bSi matrix. This can be conducted via XRF analysis ([Panizzo et al., 2018a](#)), SEM-EDS, XRD or microprobe ([Pichevin et al., 2014](#)), or ICP-OES/ICP-MS analysis after  $\text{Na}_2\text{CO}_3$  dissolution ([Ellwood and Hunter, 1999](#)) or  $\text{HCl-HNO}_3$  dissolution ([Andersen et al., 2011](#)). [Panizzo et al. \(2018a\)](#) employed a threshold  $\text{Al}_2\text{O}_3/\text{SiO}_2$  of <0.01, but in general there is no consensus on what element/Si ratio constitutes evidence of a contaminant free bSi sample. When the contaminating mineral is also relatively pure  $\text{SiO}_2$  (e.g. quartz) then elemental ratios become less useful and spectroscopic approaches (e.g. FTIR; [Swann and Patwardhan, 2011](#)) may be more appropriate. Where contaminants cannot be removed in totality, geochemical mass-balance corrections can still be employed if their  $\delta^{30}\text{Si}$  and contribution of Si to the sample is known.

In summary, we emphasise the importance of rigorous bSi

purification and species compositional analysis prior to Si isotope analysis, as well as the value of understanding the bSi preservation state (e.g. level of dissolution). The effectiveness of these methods should also be fully disclosed by authors as a means for the palaeo-community to understand the challenges and better mitigate them via method advancement. Not all samples will be challenging: it hinges on the form of bSi of interest (e.g. diatoms versus sponge spicules), the range in sizes of the species present and the composition and grain size of sediments. Indeed, the cleaning methods adopted and a good knowledge of site-specific species ecology additionally permits the ability isolate diatom species indicative of seasonal cyclicity and/or specific habitats yielding even greater knowledge of nutrient availability and utilization. Qualitative (visual) and quantitative assessments should always form a key component of any study and images and an appropriate bulk sample screening (geochemical or spectroscopic; see above) should be published to corroborate the effectiveness of cleaning. These recommendations do not act as deterrence for the application of stable Si isotopes but may help account for the recent decline in the application in Quaternary science. As a community, we hope that these challenges can be addressed and the potential for this application continues to grow, with particular focus in lacustrine environments where there remains a paucity in recently published data.

#### 6.1.1. Increasing analytical confidence in $\delta^{30}\text{Si}$ determinations

The  $\delta^{30}\text{Si}$  analysis of diatom bSi is routinely carried out via MC-ICP-

MS, instead of the more hazardous fluorination lines connected to a gas-source IRMS of early work. Indeed, the analysis of purified diatom opal via MC-ICP-MS is generally perceived to be analytically straightforward, especially when compared to e.g. marine, estuarine and freshwater dSi samples, due to the absence of complex matrix effects that are not readily removed with the common cation-exchange column chromatography methods (Gaspard et al., 2021; Georg et al., 2006; Hughes et al., 2011). Of more pressing consideration with regards to sample preparation and analysis is the availability of shared inter-laboratory calibration standards, building on the work of Reynolds et al. (2007) (and continued by Delvigne et al. (2021), and by Grasse et al. (2017) for seawater dSi samples). Indeed, there is a shortage of a previously circulated community reference material for diatom  $\delta^{30}\text{Si}$ , i.e. "Diatomite", a natural marine diatomite. This implies the need to conduct further interlaboratory-calibration exercises. Other labs may also have their own in-house standards, the sharing of which would provide greater confidence in our ability to draw comparisons between matrices, and sample preparation and analytical approaches. It is clear that a discussion is needed within the community to ensure a consensus on the future of (secondary) reference materials.

## 7. Synthesis and recommendations for future applications of $\delta^{30}\text{Si}$

We believe that diatom  $\delta^{30}\text{Si}$  is a valuable tool to decipher changes in past and present biogeochemical cycling across various space- and timescales. This is clearly not a universal belief: there has been a recent decline in publication rates in recent years (Fig. 2). One explanation for the decline is that workers are actively deterred from applying Si isotope geochemistry by a perception – whether justified or not – that  $\delta^{30}\text{Si}$  is a difficult, problematic or unreliable proxy. As the field has made progress in probing the diatom  $\delta^{30}\text{Si}$  proxy, it has inevitably highlighted challenges for the application of silicon isotope geochemistry to Quaternary research questions. Our motivation for reviewing those challenges is to question whether the scepticism is warranted, and to identify pathways towards alleviating the scepticism. We have identified four overarching challenges.

- 1. Variable silicon isotope fractionation factors (Section 3):** We observe a range in fractionation for different diatom taxa, but do not know what the dominant control on this variability is. Past changes in diatom  $\delta^{30}\text{Si}$  could therefore be influenced by changes in the diatom community, and/or environmental factors like micro-nutrient availability that modify diatom Si isotope fractionation.
- 2. Diagenetic modification of diatom  $\delta^{30}\text{Si}$  (Section 4):** Multiple processes like dissolution and exchange reactions have potential to alter the original  $\delta^{30}\text{Si}$ , either directly by adding or removing Si with a different  $\delta^{30}\text{Si}$ , or indirectly by dissolving only specific parts of the bSi. Past changes in diatom  $\delta^{30}\text{Si}$  might therefore not reflect a pristine signal.
- 3. Variable  $\delta^{30}\text{Si}$  of source dSi (Section 5):** If the relative balance of dSi inputs into a system or their  $\delta^{30}\text{Si}$  values have changed in the past, then the dSi that diatoms use to form their frustules will also change. Past changes in diatom  $\delta^{30}\text{Si}$  could therefore reflect the system's Si budget. These challenges are particularly evident for terrestrial systems which typically have short residence times.
- 4. Difficulties in isolating a pure bSi component from sediments (Section 6):** Si-bearing contaminants physically adhered to, chemically incorporated into, or not separated from, the bSi might introduce bias into  $\delta^{30}\text{Si}$  measurements. Cleaning of bSi is a challenge that is not unique to the Si isotope community. Past changes in diatom  $\delta^{30}\text{Si}$  could simply reflect the incorporation of variable amounts of 'contamination' Si into the analysis.

As outlined in the preceding sections, there are several steps that can already be taken to mitigate against these challenges. These are mostly

steps that are standard elsewhere in the palaeosciences (e.g. for foraminiferal proxies) and are not prohibitive with regards to effort or expenditure.

1. As far as possible, isolate and analyse single species, and report species assemblage changes to mitigate against e.g. seasonal, depth-habitat or species specific fractionation factors. If possible, analyse multiple taxa and/or radiolarians and sponges to (i) corroborate interpretations and (ii) demonstrate the absence of diagenetic alteration if intra-specific differences remain constant.
2. Perform a contaminant screening, e.g. analyse and report the trace-element composition of bSi or use appropriate imaging or spectroscopic techniques, to help identify diagenetic alteration and/or cleaning protocol efficacy. Document and report the cleaning steps to verify the successful exclusion of all non-bSi phases, and all unwanted bSi phases (e.g. sponge spicules, chrysophytes, etc.). If possible use  $\delta^{18}\text{O}$  to screen for recrystallisation of bSi towards opal-CT.
3. As far as possible, take a multi-proxy approach that uses other palaeoproductivity proxies (e.g. diatom-bound  $\delta^{15}\text{N}$ ), other geochemical tools (e.g. diatom Ge/Si, radiolarian  $\delta^{30}\text{Si}$ ), or quantitative palaeoecological techniques to increase confidence in interpretations.
4. If relevant, interpret records in the context of changes in regional gradients or inter-site differences in order to minimise the effects of whole system changes (cf. Dumont et al., 2020; Pichevin et al., 2020).

Beyond these easily implementable steps, there are also key knowledge gaps that need to be closed. One important question relates to what controls Si isotope fractionation by diatoms. Are the key controls biological, ecological, physical or geochemical? For this, we need both dedicated laboratory studies, and observations from both lacustrine and marine environments. A better underpinning of the fractionation process will not only help us understand the driving mechanisms, but will also open up new applications for diatom  $\delta^{30}\text{Si}$  for palaeo-reconstructions. In addition, a better understanding of the processes that influence the preservation of diatoms, and the extent, kinetics and controls of Si isotope exchange between bSi and other sediment/pore-water phases is required. Again, this will need both laboratory and field-based approaches. As suggested above, it may be prudent to look at the water column holistically, for example using multiproxy approaches and/or a combination of Si isotope proxies representing different water column levels (i.e. benthic environment – sponges, water column – radiolarians, surface – diatoms).

This review has explored the many potential factors that could explain a decline in diatom  $\delta^{30}\text{Si}$ -based Quaternary research. Given our optimism concerning the use of diatom  $\delta^{30}\text{Si}$  in marine and lacustrine environments, we wonder if the publication trends in Fig. 2 reflect another reason why the community has moved away from using diatom  $\delta^{30}\text{Si}$ . While we cannot rule out societal explanations, in particular those related to COVID-19 and associated laboratory shutdowns, we note the decline in publication rates predates the pandemic, implying an explanation rooted in scientific priorities is the key driver of the publication trends. In other words, do the publication metrics imply a loss of confidence in diatom  $\delta^{30}\text{Si}$  as a palaeo-productivity proxy, or do they instead reflect a shift in research focus? As detailed in Section 2, diatom  $\delta^{30}\text{Si}$  was conventionally used as a palaeoproductivity proxy for evaluating surface ocean dSi utilization. An outstanding problem in palaeoclimate research at the beginning of the 21st century revolved around understanding the ca. 100 ppmv increase in atmospheric pCO<sub>2</sub> from glacials into interglacials (Archer et al., 2000; Pedersen et al., 2003; Sigman and Boyle, 2000), potentially driven by changes in the strength of the biological pump or in the organic-to-inorganic carbon ratio of the export flux (Archer and Maier-Reimer, 1994). Diatom  $\delta^{30}\text{Si}$  was therefore well suited to explore how these mechanisms may have functioned

during glacial periods. They found specific use to test the so-called ‘Silicic Acid Leakage Hypothesis’ (Brzezinski et al., 2002; Nozaki and Yamamoto, 2001) and subsequent refinements (Hendry and Brzezinski, 2014; Matsumoto and Sarmiento, 2008). Ultimately, the diatom-based productivity reconstructions were equivocal about these hypotheses (Bradtmiller et al., 2006; Kienast et al., 2006). More generally, a body of work that invokes deep-sea ventilation changes driven by circulation, upwelling, stratification, or atmospheric circulation patterns seems to be rising in prominence (e.g. Gray et al., 2023). This implies that an alternative explanation for the decline in palaeo-applications of diatom  $\delta^{30}\text{Si}$  in recent years (Fig. 2) might simply reflect that the field perceives that changing diatom productivity is not relevant to understanding glacial-interglacial carbon cycle changes.

We cannot easily distinguish between the two explanations for the recent decline in  $\delta^{30}\text{Si}$  applications (i.e. distrust of the proxy *sensu lato* vs. perception that the proxy is not relevant for today’s research foci). Yet we suggest that neither is a valid reason for its reduced or discontinued use. In the first case, we have outlined above concrete steps that can already be taken to improve the robustness of Si isotope based reconstructions, and outlined knowledge gaps that can be easily filled in the coming years. In the second case, it has been convincingly argued elsewhere that the biological pump remains central to understanding CO<sub>2</sub> cycling during glacials (Galbraith and Skinner, 2020). Beyond this, we emphasise that  $\delta^{30}\text{Si}$  has utility beyond palaeoproductivity reconstructions. The development of sponge  $\delta^{30}\text{Si}$ -based [dSi] reconstructions is an excellent example of an emerging application (Fig. 3C; Hendry and Robinson, 2012). Other under-explored research directions include those that have (in)directly emerged from the extensive work trying to understand the diatom  $\delta^{30}\text{Si}$  proxy. For example, silicon isotopes have great potential to shine light on the process of silica diagenesis in general (Tatzel et al., 2024), and specifically the topic of ‘reverse weathering’, and thus the long-term carbon cycle (Geilert et al., 2023). Another exciting direction may lie in interpreting lake and ocean  $\delta^{30}\text{Si}$  records holistically as archives of catchment or continental weathering rather than ocean productivity (Frings et al., 2016). There will also be new, hard-to-predict research avenues that emerge as a result of ongoing methodological and theoretical development, including from *in-situ* microscale Si isotope analysis (Jochum et al., 2017), sample requirement miniaturisation, cosmogenic  $^{32}\text{Si}$  analyses (Rahman et al., 2017), Si isotopes as a (palaeo-)pH proxy (Fujii et al., 2015), or ‘triple’ Si isotopes to distinguish between kinetic and equilibrium isotope effects (Box 1; Pack et al., 2023; Sun et al., 2023). Overall, we envisage a bright future for Si isotope analysis in Quaternary research and look forward to seeing the field transition towards a realistic, well-grounded understanding of the diversity of applications.

#### CRediT authorship contribution statement

**Patrick J. Frings:** Conceptualization, Writing – original draft, Writing – review & editing, Visualization. **Virginia N. Panizzo:** Conceptualization, Writing – original draft, Writing – review & editing, Visualization. **Jill N. Sutton:** Conceptualization, Writing – original draft, Writing – review & editing, Visualization. **Claudia Ehlert:** Conceptualization, Writing – original draft, Writing – review & editing, Visualization.

#### Declaration of competing interest

The authors declare that they have no known competing financial interests or personal relationships that could have appeared to influence the work reported in this paper.

#### Data availability

No data was used for the research described in the article.

#### Acknowledgements

PJF acknowledges support from the GFZ Discovery Fund and thanks past and present colleagues in the HELGES (Helmholtz Laboratory for the Geochemistry of the Earth’s Surface) lab for stimulating discussions and support. We thank Sébastien Hervé (LEMAR) for his assistance in drafting Fig. 6 and Melanie Leng (BGS) for the IsoPAL initiative and the invitation to contribute to this special issue. We are grateful for constructive reviews from Kate Hendry and Jonathan Tyler on an earlier version of this manuscript.

#### References

- Abelmann, A., Gersonde, R., Knorr, G., Zhang, X., Chaplgin, B., Maier, E., Esper, O., Friedrichsen, H., Lohmann, G., Meyer, H., Tiedemann, R., 2015. The seasonal sea-ice zone in the glacial Southern Ocean as a carbon sink. *Nat. Commun.* 6.
- Akse, S.P., Middelburg, J.J., King, H.E., Polerecky, L., 2020. Rapid post-mortem oxygen isotope exchange in biogenic silica. *Geochem. Cosmochim. Acta* 284, 61–74.
- Akse, S.P., Polerecky, L., Kienhuis, M.V., Middelburg, J.J., 2022. The influence of sediment diagenesis and aluminium on oxygen isotope exchange of diatom frustules. *Geochem. Cosmochim. Acta* 333, 362–372.
- Alleman, L.Y., Cardinal, D., Cocquyt, C., Plisnier, P.D., Descy, J.P., Kimirei, I., Sinyanya, D., Andre, L., 2005. Silicon isotopic fractionation in Lake Tanganyika and its main tributaries. *J. Gt. Lakes Res.* 31, 509–519.
- Andersen, M.B., Vance, D., Archer, C., Anderson, R.F., Ellwood, M.J., Allen, C.S., 2011. The Zn abundance and isotopic composition of diatom frustules, a proxy for Zn availability in ocean surface seawater. *Earth Planet Sci. Lett.* 301, 137–145.
- Annett, A.L., Henley, S.F., Venables, H.J., Meredith, M.P., Clarke, A., Ganeshram, R.S., 2017. Silica cycling and isotopic composition in northern Marguerite Bay on the rapidly-warming western Antarctic Peninsula. *Deep Sea Res. Part II Top. Stud. Oceanogr.* 139, 132–142.
- Archer, D., Maier-Reimer, E., 1994. Effect of deep-sea sedimentary calcite preservation on atmospheric CO<sub>2</sub> Concentration. *Nature* 367, 260–263.
- Archer, D., Winguth, A., Lea, D., Mahowald, N., 2000. What caused the glacial/interglacial atmospheric pCO<sub>2</sub> cycles? *Rev. Geophys.* 38, 159–189.
- Armburst, E.V., 2009. The life of diatoms in the world’s oceans. *Nature* 459, 185–192.
- Augustin, L., Barbante, C., Barnes, P.R.F., Barnola, J.M., Bigler, M., Castellano, E., Cattani, O., Chappellaz, J., Dahl-Jensen, D., Delmonte, B., Dreyfus, G., Durand, G., Falourd, S., Fischer, H., Fluckiger, J., Hansson, M.E., Huybrechts, P., Jugie, R., Johnsen, S.J., Jouzel, J., Kaufmann, P., Kipfstuhl, J., Lambert, F., Lipenkov, V.Y., Littot, G.V.C., Longinelli, A., Lorrain, R., Maggi, V., Masson-Delmotte, V., Miller, H., Mulvaney, R., Oerlemans, J., Oerter, H., Orombelli, G., Parrenin, F., Peel, D.A., Petit, J.R., Raynaud, D., Ritz, C., Ruth, U., Schwander, J., Siegenthaler, U., Souchez, R., Stauffer, B., Steffensen, J.P., Stenni, B., Stocker, T.F., Tabacco, I.E., Udisti, R., van de Wal, R.S.W., van den Broeke, M., Weiss, J., Wilhelms, F., Winther, J.G., Wolff, E.W., Zucchielli, M., Members, E.C., 2004. Eight glacial cycles from an Antarctic ice core. *Nature* 429, 623–628.
- Baines, S.B., Twining, B.S., Brzezinski, M.A., Nelson, D.M., Fisher, N.S., 2010. Causes and biogeochemical implications of regional differences in silicification of marine diatoms. *Global Biogeochem. Cycles* 24.
- Battarbee, R., Digerfeldt, G., 1976. Palaeoecological studies of the recent development of Lake Vaxsjöön, introduction and chronology. *Arch. Hydrobiol.* 77, 330.
- Battarbee, R.W., Mackay, A.W., Jewson, D.H., Ryves, D.B., Sturm, M., 2005. Differential dissolution of Lake Baikal diatoms: correction factors and implications for palaeoclimatic reconstruction. *Global Planet. Change* 46, 75–86.
- Beucher, C.P., Brzezinski, M.A., Jones, J.L., 2008. Sources and biological fractionation of silicon isotopes in the eastern equatorial pacific. *Geochem. Cosmochim. Acta* 72, 3063–3073.
- Beucher, C.P., Brzezinski, M.A., Jones, J.L., 2011. Mechanisms controlling silicon isotope distribution in the Eastern Equatorial Pacific. *Geochem. Cosmochim. Acta* 75, 4286–4294.
- Bidle, K.D., Azam, F., 1999. Accelerated dissolution of diatom silica by marine bacterial assemblages. *Nature* 397, 508–512.
- Bidle, K.D., Brzezinski, M.A., Long, R.A., Jones, J.L., Azam, F., 2003. Diminished efficiency in the oceanic silica pump caused by bacteria-mediated silica dissolution. *Limnol. Oceanogr.* 48, 1855–1868.
- Bishop, J.K., Biscaye, P.E., 1982. Chemical characterization of individual particles from the nepheloid layer in the Atlantic Ocean. *Earth Planet Sci. Lett.* 58, 265–275.
- Boutorh, J., Moriceau, B., Gallinari, M., Ragueneau, O., Buccarelli, E., 2016. Effect of trace metal-limited growth on the postmortem dissolution of the marine diatom *Pseudo-nitzschia delicatissima*. *Global Biogeochem. Cycles* 30, 57–69.
- Bradtmiller, L.I., Anderson, R.F., Fleisher, M.Q., Burckle, L.H., 2006. Diatom productivity in the equatorial Pacific Ocean from the last glacial period to the present: a test of the silicic acid leakage hypothesis. *Paleoceanography* 21.
- Brzezinski, M.A., Jones, J.L., 2015. Coupling of the distribution of silicon isotopes to the meridional overturning circulation of the North Atlantic Ocean. *Deep Sea Res. Part II Top. Stud. Oceanogr.* 116, 79–88.
- Brzezinski, M.A., Pride, C.J., Franck, V.M., Sigman, D.M., Sarmiento, J.L., Matsumoto, K., Gruber, N., Rau, G.H., Coale, K.H., 2002. A switch from Si(OH)<sub>4</sub> to NO<sub>3</sub><sup>-</sup> depletion in the glacial Southern Ocean. *Geophys. Res. Lett.* 29.

- Cao, Z., Frank, M., Dai, M., 2015. Dissolved silicon isotopic compositions in the E ast C hina S ea: water mass mixing vs. biological fractionation. *Limnol. Oceanogr.* 60, 1619–1633.
- Cao, Z., Frank, M., Dai, M., Grasse, P., Ehler, C., 2012. Silicon isotope constraints on sources and utilization of silicic acid in the northern South China Sea. *Geochem. Cosmochim. Acta* 97, 88–104.
- Cardinal, D., Alleman, L.Y., Dehairs, F., Savoye, N., Trull, T.W., André, L., 2005. Relevance of silicon isotopes to Si-nutrient utilization and Si-source assessment in Antarctic waters. *Global Biogeochem. Cycles* 19, GB2007.
- Cardinal, D., Savoye, N., Trull, T.W., Dehairs, F., Kopczynska, E.E., Fripiat, F., Tison, J., André, L., 2007. Silicon isotopes in spring Southern Ocean diatoms: large zonal changes despite homogeneity among size fractions. *Mar. Chem.* 106, 46.
- Cassarino, L., Coath, C.D., Xavier, J.R., Hendry, K.R., 2018. Silicon isotopes of deep sea sponges: new insights into biomineralisation and skeletal structure. *Biogeosciences* 15, 6959–6977.
- Cassarino, L., Curnow, P., Hendry, K.R., 2021. A biomimetic peptide has no effect on the isotopic fractionation during in vitro silica precipitation. *Sci. Rep.* 11, 9698.
- Cassarino, L., Hendry, K.R., Meredith, M.P., Venables, H.J., De La Rocha, C.L., 2017. Silicon isotope and silicic acid uptake in surface waters of Marguerite Bay, West Antarctic Peninsula. *Deep Sea Res. Part II Top. Stud. Oceanogr.* 139, 143–150.
- Cavagna, A.J., Fripiat, F., Dehairs, F., Wolf-Gladrow, D., Cisewski, B., Savoye, N., André, L., Cardinal, D., 2011. Silicon uptake and supply during a Southern Ocean iron fertilization experiment (EIFEX) tracked by Si isotopes. *Limnol. Oceanogr.* 56, 147–160.
- Chakrabarti, R., Knoll, A.H., Jacobsen, S.B., Fischer, W.W., 2012. Si isotope variability in Proterozoic cherts. *Geochem. Cosmochim. Acta* 91, 187–201.
- Charlet, L., Manceau, A., 1994. Evidence for the neoformation of clays upon sorption of Co (II) and Ni (II) on silicates. *Geochem. Cosmochim. Acta* 58, 2577–2582.
- Chase, Z., Ellwood, M.J., van de Flierdt, T., 2018. Discovering the ocean's past through geochemistry. *Elements: An International Magazine of Mineralogy, Geochemistry, and Petrology* 14, 397–402.
- Cheng, T., Hammond, D.E., Berelson, W.M., Hering, J.G., Dixit, S., 2009. Dissolution kinetics of biogenic silica collected from the water column and sediments of three Southern California borderland basins. *Mar. Chem.* 113, 41–49.
- Chu, J.W., Maldonado, M., Yahel, G., Leys, S.P., 2011. Glass sponge reefs as a silicon sink. *Mar. Ecol. Prog. Ser.* 441, 1–14.
- Closset, I., Brzezinski, M.A., Cardinal, D., Dapoigny, A., Jones, J.L., Robinson, R.S., 2022. A silicon isotopic perspective on the contribution of diagenesis to the sedimentary silicon budget in the Southern Ocean. *Geochem. Cosmochim. Acta* 327, 298–313.
- Closset, I., Cardinal, D., Bray, S.G., Thil, F., Djouraev, I., Rigual-Hernández, A.S., Trull, T. W., 2015. Seasonal variations, origin, and fate of settling diatoms in the Southern Ocean tracked by silicon isotope records in deep sediment traps. *Global Biogeochem. Cycles* 29, 1495–1510.
- Closset, I., Cardinal, D., Rembauville, M., Thil, F., Blain, S., 2016. Unveiling the Si cycle using isotopes in an iron-fertilized zone of the Southern Ocean: from mixed-layer supply to export. *Biogeosciences* 13, 6049–6066.
- Closset, I., Cardinal, D., Trull, T.W., Fripiat, F., 2019. New insights into processes controlling the 630Si of sinking diatoms: a seasonally resolved box model approach. *Global Biogeochem. Cycles* 33, 957–970.
- Cockerton, H.E., Street-Perrott, F.A., Barker, P.A., Leng, M.J., Sloane, H.J., Ficken, K.J., 2015. Orbital forcing of glacial/interglacial variations in chemical weathering and silicon cycling within the upper White Nile basin, East Africa: stable-isotope and biomarker evidence from Lakes Victoria and Edward. *Quat. Sci. Rev.* 130, 57–71.
- Coffineau, N., De La Rocha, C.L., Pondaven, P., 2014. Exploring interacting influences on the silicon isotopic composition of the surface ocean: a case study from the Kerguelan Plateau. *Biogeosciences* 11, 1371–1391.
- Conley, D.J., 2002. Terrestrial ecosystems and the global biogeochemical silica cycle. *Global Biogeochem. Cycles* 16, 8.
- Conley, D.J., Schelske, C.L., 1993. Potential role of sponge spicules in influencing the silicon biogeochemistry of Florida lakes. *Can. J. Fish. Aquat. Sci.* 50, 296–302.
- Criss, R.E., 1999. Principles of Stable Isotope Distribution.
- De la Rocha, C.L., 2002. Measurement of silicon stable isotope natural abundances via multicollector inductively coupled plasma mass spectrometry (MC-ICP-MS). *G-cubed* 3, 1–8.
- De La Rocha, C.L., 2003. Silicon isotope fractionation by marine sponges and the reconstruction of the silicon isotope composition of ancient deep water. *Geology* 31, 423–426.
- De La Rocha, C.L., 2006. The biological pump. *The Oceans and Marine Geochemistry* 6, 83–112.
- De La Rocha, C.L., Brzezinski, M.A., DeNiro, M.J., 1996. Purification, recovery, and laser-driven fluorination of silicon from dissolved and particulate silica for the measurement of natural stable isotope abundances. *Anal. Chem.* 68, 3746–3750.
- De La Rocha, C.L., Brzezinski, M.A., DeNiro, M.J., 1997a. Fractionation of silicon isotopes by marine diatoms during biogenic silica formation. *Geochem. Cosmochim. Acta* 61, 5051–5056.
- De La Rocha, C.L., Brzezinski, M.A., DeNiro, M.J., 1997b. Fractionation of silicon isotopes by marine diatoms during biogenic silica formation. *Geochem. Cosmochim. Acta* 61, 5051.
- De La Rocha, C.L., Brzezinski, M.A., DeNiro, M.J., 2000. A first look at the distribution of the stable isotopes of silicon in natural waters. *Geochem. Cosmochim. Acta* 64, 2467–2477.
- De La Rocha, C.L., Brzezinski, M.A., DeNiro, M.J., Shemesh, A., 1998. Silicon-isotope composition of diatoms as an indicator of past oceanic change. *Nature* 395, 680–683.
- de Souza, G.F., Reynolds, B.C., Johnson, G.C., Bullister, J.L., Bourdon, B., 2012a. Silicon stable isotope distribution traces Southern Ocean export of Si to the eastern South Pacific thermocline. *Biogeosciences* 9, 4199–4213.
- de Souza, G.F., Reynolds, B.C., Rickli, J., Frank, M., Saito, M.A., Gerrings, L.J.A., Bourdon, B., 2012b. Southern Ocean control of silicon stable isotope distribution in the deep Atlantic Ocean. *Global Biogeochem. Cycles* 26, GB2035.
- de Souza, G.F., Slater, R.D., Hain, M.P., Brzezinski, M.A., Sarmiento, J.L., 2015. Distal and proximal controls on the silicon stable isotope signature of North Atlantic Deep Water. *Earth Planet. Sci. Lett.* 432, 342–353.
- Debyser, M.C., Pichevin, L., Tueraea, R.E., Dodd, P.A., Doncila, A., Ganeshram, R.S., 2022. Tracing the role of Arctic shelf processes in Si and N cycling and export through the Fram Strait: insights from combined silicon and nitrate isotopes. *Biogeosciences* 19, 5499–5520.
- Delstanche, S., Opfergelt, S., Cardinal, D., Elsass, F., André, L., Delvaux, B., 2009. Silicon isotopic fractionation during adsorption of aqueous monosilicic acid onto iron oxide. *Geochem. Cosmochim. Acta* 73, 923–934.
- Delvigne, C., Guihou, A., Schuessler, J.A., Savage, P., Poitrasson, F., Fischer, S., Hatton, J.E., Hendry, K.R., Bayon, G., Ponzevera, E., 2021. Silicon isotope analyses of soil and plant reference materials: an inter-comparison of seven laboratories. *Geostand. Geoanal. Res.* 45, 525–538.
- Demarest, M.S., Brzezinski, M.A., Beucher, C.P., 2009. Fractionation of silicon isotopes during biogenic silica dissolution. *Geochem. Cosmochim. Acta* 73, 5572–5583.
- Devi, R., 2023. Using Silicon Isotopes to Trace the Biogenic Silica in the Southern Ocean. *Australasian National University*.
- Dixit, S., Van Cappellen, P., van Bennekom, A.J., 2001. Processes controlling solubility of biogenic silica and pore water build-up of silicic acid in marine sediments. *Mar. Chem.* 73, 333–352.
- Dodd, J.P., Wiedenheft, W., Schwartz, J.M., 2017. Dehydroxylation and diagenetic variations in diatom oxygen isotope values. *Geochem. Cosmochim. Acta* 199, 185–195.
- Doering, K., Ehler, C., Grasse, P., Crosta, X., Fleury, S., Frank, M., Schneider, R., 2016. Differences between mono-generic and mixed diatom silicon isotope compositions trace present and past nutrient utilisation off Peru. *Geochem. Cosmochim. Acta* 177, 30–47.
- Doering, K., Ehler, C., Pahnke, K., Frank, M., Schneider, R., Grasse, P., 2021. Silicon isotope signatures of radiolaria reveal taxon-specific differences in isotope fractionation. *Front. Mar. Sci.* 8, 666896. Art. Nr.
- Dove, P.M., 1994. The dissolution kinetics of quartz in sodium chloride solutions at 25 degrees to 300 degrees C. *Am. J. Sci.* 294, 665–712.
- Dove, P.M., Crerar, D.A., 1990. Kinetics of quartz dissolution in electrolyte solutions using a hydrothermal mixed flow reactor. *Geochem. Cosmochim. Acta* 54, 955–969.
- Dove, P.M., Elston, S.F., 1992. Dissolution kinetics of quartz in sodium chloride solutions: analysis of existing data and a rate model for 25°C. *Geochem. Cosmochim. Acta* 56, 4147–4156.
- Dumont, M., Pichevin, L., Geibert, W., Crosta, X., Michel, E., Moreton, S., Dobby, K., Ganeshram, R., 2020. The nature of deep overturning and reconfigurations of the silicon cycle across the last deglaciation. *Nat. Commun.* 11, 1–11.
- Dupuis, R., Benoit, M., Nardin, E., Méheut, M., 2015. Fractionation of silicon isotopes in liquids: the importance of configurational disorder. *Chem. Geol.* 396, 239–254.
- Dutkiewicz, A., O'Callaghan, S., Müller, R.D., 2016. Controls on the distribution of deep-sea sediments. *G-cubed* 17, 3075–3098.
- Egan, K.E., Rickaby, R.E.M., Leng, M.J., Hendry, K.R., Hermoso, M., Sloane, H.J., Bostock, H., Halliday, A.N., 2012. Diatom silicon isotopes as a proxy for silicic acid utilisation: a Southern Ocean core top calibration. *Geochem. Cosmochim. Acta* 96, 174–192.
- Ehler, C., Doering, K., Wallmann, K., Scholz, F., Sommer, S., Grasse, P., Geilert, S., Frank, M., 2016. Stable silicon isotope signatures of marine pore waters – biogenic opal dissolution versus authigenic clay mineral formation. *Geochem. Cosmochim. Acta* 191, 102–117.
- Ehler, C., Grasse, P., Mollier-Vogel, E., Bösch, T., Franz, J., de Souza, G.F., Reynolds, B.C., Stramma, L., Frank, M., 2012. Factors controlling the silicon isotope distribution in waters and surface sediments of the Peruvian coastal upwelling. *Geochem. Cosmochim. Acta* 99, 128–145.
- Ehrenhauss, S., Witte, U., Janssen, F., Huettel, M., 2004. Decomposition of diatoms and nutrient dynamics in permeable North Sea sediments. *Cont. Shelf Res.* 24, 721–737.
- Elderfield, H., 2002. Foraminiferal Mg/Ca paleothermometry: expected advances and unexpected consequences. *Geochimica et Cosmochimica Acta. PERGAMON-ELSEVIER SCIENCE LTD THE BOULEVARD, LANGFORD LANE, KIDLINGTON, p. A213. A213.*
- Ellwood, M.J., Hunter, K.A., 1999. Determination of the Zn/Si ratio in diatom opal: a method for the separation, cleaning and dissolution of diatoms. *Mar. Chem.* 66, 149–160.
- Etourneau, J., Ehler, C., Frank, M., Martinez, P., Schneider, R., 2012. Contribution of changes in opal productivity and nutrient distribution in the coastal upwelling systems to Late Pliocene/Early Pleistocene climate cooling. *Clim. Past.* 8, 1435–1445.
- Farmer, J.R., Hertzberg, J., Cardinal, D., Fietz, S., Hendry, K., Jaccard, S., Paytan, A., Rafter, P., Ren, H., Somes, C.J., 2021. Assessment of C, N, and Si Isotopes as Tracers of Past Ocean Nutrient and Carbon Cycling. *Wiley Online Library*.
- Fernandez, N.M., Zhang, X., Druhan, J.L., 2019. Silicon isotopic re-equilibration during amorphous silica precipitation and implications for isotopic signatures in geochemical proxies. *Geochem. Cosmochim. Acta* 262, 104–127.
- Fontorbe, G., Frings, P.J., Christina, L., Hendry, K.R., Carstensen, J., Conley, D.J., 2017. Enrichment of dissolved silica in the deep equatorial Pacific during the Eocene–Oligocene. *Paleoceanography* 32, 848–863.
- Fortin, M.C., Gajewski, K., 2009. Assessing the use of sediment organic, carbonate and biogenic silica content as indicators of environmental conditions in Arctic lakes. *Polar Biol.* 32, 985–998.

- Frings, P.J., 2017. Revisiting the dissolution of biogenic Si in marine sediments: a key term in the ocean Si budget. *Acta Geochimica* 36, 429–432.
- Frings, P.J., Clymans, W., Jeppesen, E., Lauridsen, T.L., Struyf, E., Conley, D.J., 2014a. Lack of steady-state in the global biogeochemical Si cycle: emerging evidence from lake Si sequestration. *Biogeochemistry* 117, 255–277.
- Frings, P.J., De La Rocha, C., Struyf, E., van Pelt, D., Schoelynck, J., Hudson, M.M., Gondwe, M.J., Wolski, P., Mosimane, K., Gray, W., Schaller, J., Conley, D.J., 2014b. Tracing silicon cycling in the Okavango Delta, a sub-tropical flood-pulse wetland using silicon isotopes. *Geochem. Cosmochim. Acta* 142, 132–148.
- Frings, P.J., Fontorbe, G., Clymans, W., De La Rocha, C.L., Conley, D.J., 2016. The continental Si cycle and its impact on the ocean Si isotope budget. *Chem. Geol.* 425, 12–36.
- Frings, P.J., Oelze, M., Schubring, F., Frick, D.A., von Blanckenburg, F., 2021. Interpreting silicon isotopes in the critical zone. *Am. J. Sci.* 321, 1164–1203.
- Fripia, F., Cardinal, D., Tison, J.L., Worby, A., André, L., 2007. Diatom-induced silicon isotopic fractionation in Antarctic sea ice. *J. Geophys. Res.: Biogeosciences* 112.
- Fripia, F., Cavagna, A.-J., Dehairs, F., De Brauwere, A., André, L., Cardinal, D., 2012. Processes controlling the Si-isotopic composition in the Southern Ocean and application for paleoceanography. *Biogeosciences* 9, 2443–2457.
- Fripia, F., Cavagna, A.-J., Savoye, N., Dehairs, F., André, L., Cardinal, D., 2011a. Isotopic constraints on the Si-biogeochemical cycle of the antarctic zone in the kerguelen area (KEOPS). *Mar. Chem.* 123, 11–22.
- Fripia, F., Cavagna, A.-J., Savoye, N., Dehairs, F., Andre, L., Cardinal, D., 2011b. Isotopic constraints on the Si-biogeochemical cycle of the antarctic zone in the kerguelen area (KEOPS). *Mar. Chem.* 123, 11–22.
- Fujii, T., Pringle, E.A., Chaussidon, M., Moynier, F., 2015. Isotope fractionation of Si in protonation/deprotonation reaction of silicic acid: a new pH proxy. *Geochem. Cosmochim. Acta* 168, 193–205.
- Galbraith, E.D., Skinner, L.C., 2020. The biological pump during the last glacial maximum. *Ann. Rev. Mar. Sci.* 12, 559–586.
- Gallinari, M., Ragueneau, O., Corrin, L., DeMaster, D.J., Treguer, P., 2002. The importance of water column processes on the dissolution properties of biogenic silica in deep-sea sediments I. Solubility. *Geochem. Cosmochim. Acta* 66, 2701–2717.
- Gaspard, F., Opfergelt, S., Hirst, C., Hurwitz, S., McCleskey, R.B., Zahajská, P., Conley, D.J., Delmelle, P., 2021. Quantifying non-thermal silicate weathering using Ge/Si and Si isotopes in rivers draining the Yellowstone plateau volcanic field, USA. *G-cubed* 22, e2021GC009904.
- Gehlen, M., Van Raaphorst, W., 2002. The role of adsorption-desorption surface reactions in controlling interstitial Si(OH)(4) concentrations and enhancing Si(OH)(4) turnover in shallow shelf seas. *Cont. Shelf Res.* 22, 1529–1547.
- Geilert, S., Frick, D.A., Garbe-Schönberg, D., Scholz, F., Sommer, S., Grasse, P., Vogt, C., Dale, A.W., 2023. Coastal El Niño triggers rapid marine silicate alteration on the seafloor. *Nat. Commun.* 14, 1676.
- Geilert, S., Grasse, P., Doering, K., Wallmann, K., Ehlert, C., Scholz, F., Frank, M., Schmidt, M., Hensen, C., 2020. Impact of ambient conditions on the Si isotope fractionation in marine pore fluids during early diagenesis. *Biogeosciences* 17, 1745–1763.
- Geilert, S., Vroon, P.Z., Roerdink, D.L., Cappellen, P.V., van Bergen, M.J., 2014. Silicon isotope fractionation during abiotic silica precipitation at low temperatures: inferences from flow-through experiments. *Geochem. Cosmochim. Acta* 142, 95–114.
- Gendron-Badou, A., Coradin, T., Maquet, J., Frohlich, F., Livage, J., 2003. Spectroscopic characterization of biogenic silica. *J. Non-Cryst. Solids* 316, 331–337.
- Georg, R.B., Reynolds, B.C., Frank, M., Halliday, A.N., 2006. New sample preparation techniques for the determination of Si isotopic compositions using MC-ICPMS. *Chem. Geol.* 235, 95.
- Georg, R.B., West, A.J., Basu, A.R., Halliday, A.N., 2009a. Silicon fluxes and isotope composition of direct groundwater discharge into the Bay of Bengal and the effect on the global ocean silicon isotope budget. *Earth Planet Sci. Lett.* 283, 67.
- Georg, R.B., Zhu, C., Reynolds, B.C., Halliday, A.N., 2009b. Stable silicon isotopes of groundwater, feldspars, and clay coatings in the Navajo Sandstone aquifer, Black Mesa, Arizona, USA. *Geochem. Cosmochim. Acta* 73, 2229–2241.
- Gouretski, V., Koltermann, K.P., 2004. WOCE global hydrographic climatology. *Berichte des BSH* 35, 1–52.
- Grasse, P., Brzezinski, M.A., Cardinal, D., de Souza, G.F., Andersson, P., Closset, I., Cao, Z., Dai, M., Ehlert, C., Estrade, N., Francois, R., Frank, M., Jiang, G., Jones, J.L., Kooijman, E., Liu, Q., Lu, D., Pahnke, K., Ponzevera, E., Schmitt, M., Sun, X., Sutton, J.N., Thil, F., Weis, D., Wetzel, F., Zhang, A., Zhang, J., Zhang, Z., 2017. GEOTRACES inter-calibration of the stable silicon isotope composition of dissolved silicic acid in seawater. *Journal of Analytical Atomic Spectrometry* 32 (3), 562–578.
- Grasse, P., Closset, I., Jones, J., Geilert, S., Brzezinski, M., 2020. Controls on dissolved silicon isotopes along the US GEOTRACES eastern pacific zonal transect (GP16). *Global Biogeochem. Cycles* 34, e2020GB006538.
- Grasse, P., Ehlert, C., Frank, M., 2013. The influence of water mass mixing on the dissolved Si isotope composition in the Eastern Equatorial Pacific. *Earth Planet Sci. Lett.* 380, 60–71.
- Grasse, P., Haynert, K., Doering, K., Geilert, S., Jones, J.L., Brzezinski, M.A., Frank, M., 2021a. Controls on the silicon isotope composition of diatoms in the peruvian upwelling. *Front. Mar. Sci.* 8, 697400.
- Grasse, P., Haynert, K., Doering, K., Geilert, S., Jones, J.L., Brzezinski, M.A., Frank, M., 2021b. Controls on the silicon isotope composition of diatoms in the Peruvian upwelling. *Front. Mar. Sci.* 8.
- Gray, W.R., de Lavergne, C., Jinglin Wills, R.C., Menviel, L., Spence, P., Holzer, M., Kageyama, M., Michel, E., 2023. Poleward shift in the southern hemisphere westerly winds synchronous with the deglacial rise in CO<sub>2</sub>. *Paleoceanogr. Paleoclimatol.* 38, e2023PA00466.
- Griffin, J.J., Windom, H., Goldberg, E.D., 1968. The distribution of clay minerals in the world ocean. *Deep Sea Research and Oceanographic Abstracts* 433–459. Elsevier.
- Griffiths, J.D., Barker, S., Hendry, K.R., Thornalley, D.J.R., van de Flierdt, T., Hall, I.R., Anderson, R.F., 2013. Evidence of silicic acid leakage to the tropical atlantic via antarctic intermediate water during marine isotope stage 4. *Paleoceanography* 28, 307–318.
- Harrison, K.G., 2000. Role of increased marine silica input on paleo-pCO<sub>2</sub> levels. *Paleoceanography* 15, 292–298.
- Hatton, J., Ng, H., Meire, L., Woodward, E., Leng, M., Coath, C., Stuart-Lee, A., Wang, T., Annett, A., Hendry, K., 2023. Silicon isotopes highlight the role of glaciated fjords in modifying coastal waters. *J. Geophys. Res.: Biogeosciences*, e2022JG007242.
- Hatton, J.E., Hendry, K.R., Hawkins, J.R., Wadham, J.L., Opfergelt, S., Kohler, T.J., Yde, J.C., Stibal, M., Žářský, J.D., 2019. Silicon isotopes in Arctic and sub-Arctic glacial meltwaters: the role of subglacial weathering in the silicon cycle. *Proceedings of the Royal Society A* 475, 20190098.
- Heathcote, A.J., Hobbs, J.M.R., Anderson, N.J., Frings, P., Engstrom, D.R., Downing, J. A., 2015. Diatom floristic change and lake paleoproduction as evidence of recent eutrophication in shallow lakes of the midwestern USA. *J. Paleolimnol.* 53, 17–34.
- Hecky, R., Mopper, K., Kilham, P., Degens, E., 1973. The amino acid and sugar composition of diatom cell-walls. *Marine biology* 19, 323–331.
- Hendry, K.R., Romero, O., Pashley, V., 2021. Nutrient utilization and diatom productivity changes in the low-latitude south-eastern Atlantic over the past 70 ka: response to Southern Ocean leakage. *Clim. Past* 17, 603–614.
- Hendry, K.R., Brzezinski, M.A., 2014. Using silicon isotopes to understand the role of the Southern Ocean in modern and ancient biogeochemistry and climate. *Quat. Sci. Rev.* 89, 13–26.
- Hendry, K.R., Cassarino, L., Bates, S.L., Culwick, T., Frost, M., Goodwin, C., Howell, K.L., 2019. Silicon isotopic systematics of deep-sea sponge grounds in the North Atlantic. *Quat. Sci. Rev.* 210, 1–14.
- Hendry, K.R., Georg, R.B., Rickaby, R.E.M., Robinson, L.F., Halliday, A.N., 2010. Deep ocean nutrients during the Last Glacial Maximum deduced from sponge silicon isotopic compositions. *Earth Planet Sci. Lett.* 292, 290–300.
- Hendry, K.R., Gong, X., Knorr, G., Pike, J., Hall, I.R., 2016. Deglacial diatom production in the tropical North Atlantic driven by enhanced silicic acid supply. *Earth Planet Sci. Lett.* 438, 122–129.
- Hendry, K.R., Robinson, L.F., 2012. The relationship between silicon isotope fractionation in sponges and silicic acid concentration: modern and core-top studies of biogenic opal. *Geochem. Cosmochim. Acta* 81, 1–12.
- Hendry, K.R., Robinson, L.F., McManus, J.F., Hays, J.D., 2014. Silicon isotopes indicate enhanced carbon export efficiency in the North Atlantic during deglaciation. *Nat. Commun.* 5.
- Hendry, K.R., Robinson, L.F., Meredith, M.P., Mulitza, S., Chiessi, C.M., Arz, H., 2012. Abrupt changes in high-latitude nutrient supply to the Atlantic during the last glacial cycle. *Geology* 40, 123–126.
- Hendry, K.R., Swann, G.E.A., Leng, M.J., Sloane, H.J., Goodwin, C., Berman, J., Maldonado, M., 2015. Technical Note: silica stable isotopes and silicification in a carnivorous sponge *Asbestopluma* sp. *Biogeosciences* 12, 3489–3498.
- Hildebrand, M., Lerch, S.J.L., Shrestha, R.P., 2018. Understanding diatom cell wall silicification—moving forward. *Front. Mar. Sci.* 5.
- Holzer, M., Brzezinski, M.A., 2015. Controls on the silicon isotope distribution in the ocean: new diagnostics from a data-constrained model. *Global Biogeochem. Cycles* 29, 267–287.
- Huang, T.-H., Sun, X., Somelar, P., Kirsimäe, K., Pickering, R.A., Kim, J.-H., Kielman-Schmitt, M., Hong, W.-L., 2023. Separating Si phases from diagenetically-modified sediments through sequential leaching. *Chem. Geol.* 637, 121681.
- Hughes, H.J., Delvigne, C., Kornthauer, M., de Jong, J., Andre, L., Cardinal, D., 2011. Controlling the mass bias introduced by anionic and organic matrices in silicon isotopic measurements by MC-ICP-MS. *Journal of Analytical Atomic Spectrometry* 26, 1892–1896.
- Hurd, D.C., 1972. Factors affecting solution rate of biogenic opal in seawater. *Earth Planet Sci. Lett.* 15, 411–417.
- Hurd, D.C., 1973. Interactions of biogenic opal, sediment and seawater in the Central Equatorial Pacific. *Geochem. Cosmochim. Acta* 37, 2257–2282.
- Ibarra, D.E., Yanchilina, A.G., Lloyd, M.K., Methner, K.A., Chamberlain, C.P., Yam, R., Shemesh, A., Stolper, D.A., 2022. Triple oxygen isotope systematics of diagenetic recrystallization of diatom opal-A to opal-CT to microquartz in deep sea sediments. *Geochem. Cosmochim. Acta* 320, 304–323.
- Iler, K.R., 1979. *The Chemistry of Silica*.
- Jansen, J.F., van der Gaast, S.J., 1988. Accumulation and dissolution of opal in Quaternary sediments of the Zaire deep-sea fan (northeastern Angola Basin). *Mar. Geol.* 83, 1–7.
- Jochum, K., Schuessler, J., Wang, X.H., Stoll, B., Weis, U., Müller, W., Haug, G., Andreea, M., Froelich, P., 2017. Whole-Ocean changes in silica and Ge/Si ratios during the last deglacial deduced from long-lived giant glass sponges. *Geophys. Res. Lett.* 44.
- Johnson, T.C., 1976. Controls on the preservation of biogenic opal in sediments of the eastern tropical Pacific. *Science* 192, 887–890.
- Johnson, T.C., Brown, E.T., Shi, J.M., 2011. Biogenic silica deposition in Lake Malawi, East Africa over the past 150,000 years. *Palaeogeogr. Palaeoclimatol. Palaeoecol.* 303, 103–109.
- Jones, B.F., Weir, A.H., 1983. Clay minerals of lake aberl, an alkaline, saline lake. *Clay Clay Miner.* 31, 161–172.
- Juillet-Leclerc, A., 1986. Cleaning process for diatomaceous samples. In: Ricard, M. (Ed.), *Proceedings of the 8th Diatom Symposium*. Koeltz Scientific Books, Koenigstein, pp. 733–736.

- Kamatani, A., 1982. Dissolution rates of silica from diatoms decomposing at various temperatures. *Marine Biology* 68, 91–96.
- Kamatani, A., Ejiri, N., Treguer, P., 1988. The dissolution kinetics of diatom ooze from the Antarctic area. *Deep Sea Research Part A. Oceanographic Research Papers* 35, 1195–1203.
- Katz, M.E., Wright, J.D., Miller, K.G., Cramer, B.S., Fennel, K., Falkowski, P.G., 2005. Biological overprint of the geological carbon cycle. *Mar. Geol.* 217, 323–338.
- Kiczka, M., Wiederhold, J.G., Frommer, J., Kraemer, S.M., Bourdon, B., Kretzschmar, R., 2010. Iron isotope fractionation during proton-and ligand-promoted dissolution of primary phyllosilicates. *Geochem. Cosmochim. Acta* 74, 3112–3128.
- Kienast, S.S., Kienast, M., Jaccard, S., Calvert, S.E., Francois, R., 2006. Testing the silica leakage hypothesis with sedimentary opal records from the eastern equatorial Pacific over the last 150 kyr. *Geophys. Res. Lett.* 33.
- Kim, S., Khim, B.-K., 2017. Estimate of glacial silicic acid reduction over the last 600 ka in the Bering Sea using  $^{83}\text{Si}$  of diatom frustules. *Geochem. J.* 51, 347–357.
- Knoll, A.H., 2003. Biomineralization and evolutionary history. *Rev. Mineral. Geochem.* 54, 329–356.
- Koning, E., Gehlen, M., Flank, A.-M., Calas, G., Epping, E., 2007. Rapid post-mortem incorporation of aluminum in diatom frustules: evidence from chemical and structural analyses. *Mar. Chem.* 106, 208–222.
- Laukert, G., Grasse, P., Novikhin, A., Povazhnyi, V., Doering, K., Hölemann, J., Janout, M., Bauch, D., Kassens, H., Frank, M., 2022. Nutrient and silicon isotope dynamics in the laptev sea and implications for nutrient availability in the transpolar drift. *Global Biogeochem. Cycles* 36, e2022GB007316.
- Lazarus, D.B., Kotre, B., Wulf, G., Schmidt, D.N., 2009. Radiolarians Decreased Silicification as an Evolutionary Response to Reduced Cenozoic Ocean Silica Availability, vol. 106. Proceedings of the National Academy of Sciences, pp. 9333–9338.
- Leclerc, A.J., Labeyrie, L., 1987. Temperature dependence of the oxygen isotopic fractionation between diatom silica and water. *Earth Planet Sci. Lett.* 84, 69–74.
- Lewin, J.C., 1961. The dissolution of silica from diatom walls. *Geochem. Cosmochim. Acta* 21, 182–198.
- Leynaert, A., Bucciarelli, E., Clauquin, P., Dugdale, R.C., Martin-Jézéquel, V., Pondaven, P., Ragueneau, O., 2004. Effect of iron deficiency on diatom cell size and silicic acid uptake kinetics. *Limnol. Oceanogr.* 49, 1134–1143.
- Leynaert, A., Fardel, C., Beker, B., Soler, C., Delebecq, G., Lemercier, A., Pondaven, P., Durand, P., Heggarty, K., 2018. Diatom frustules nanostructure in pelagic and benthic environments. *Silicon* 10, 2701–2709.
- Li, Y., Ding, T., Wan, D., 1995. Experimental study of silicon isotope dynamic fractionation and its application in geology. *Chin. J. Geochem.* 14, 212–219.
- Liesegang, M., Tomaschek, F., 2020. Tracing the continental diagenetic loop of the opal-A to opal-CT transformation with X-ray diffraction. *Sediment. Geol.* 398, 105603.
- Liu, D., Tian, Q., Li, M., Mi, M., Yuan, P., Yu, R., Zhou, J., Du, P., Wei, H., Guo, H., 2024. Coupled Si-Al biogeochemistry: occurrence of aluminum in diatom-derived biogenic silica. *J. Geophys. Res.: Biogeosciences* 129, e2023JG007467.
- Liu, D., Yuan, P., Tian, Q., Liu, H., Deng, L., Song, Y., Zhou, J., Losic, D., Zhou, J., Song, H., Guo, H., Fan, W., 2019. Lake sedimentary biogenic silica from diatoms constitutes a significant global sink for aluminium. *Nat. Commun.* 10, 4829.
- Llopis Monferrer, N., Boltovskoy, D., Tréguer, P., Sandin, M.M., Not, F., Leynaert, A., 2020. Estimating biogenic silica production of Rhizaria in the global ocean. *Global Biogeochem. Cycles* 34, e2019GB006286.
- Loucaides, S., Behrends, T., Van Cappellen, P., 2010a. Reactivity of biogenic silica: surface versus bulk charge density. *Geochem. Cosmochim. Acta* 74, 517–530.
- Loucaides, S., Cappellen, P., Roubeix, V., Moriceau, B., Ragueneau, O., 2012a. Controls on the recycling and preservation of biogenic silica from biomineralization to burial. *Silicon* 4, 7–22.
- Loucaides, S., Koning, E., Van Cappellen, P., 2012b. Effect of pressure on silica solubility of diatom frustules in the oceans: results from long-term laboratory and field incubations. *Mar. Chem.* 136–137, 1–6.
- Loucaides, S., Michalopoulos, P., Presti, M., Koning, E., Behrends, T., Van Cappellen, P., 2010b. Seawater-mediated interactions between diatomaceous silica and terrigenous sediments: results from long-term incubation experiments. *Chem. Geol.* 270, 68–79.
- Loucaides, S., Van Cappellen, P., Behrends, T., 2008. Dissolution of biogenic silica from land to ocean: role of salinity and pH. *Limnol. Oceanogr.* 53, 1614–1621.
- Luo, M., Li, W., Geilert, S., Dale, A.W., Song, Z., Chen, D., 2022. Active silica diagenesis in the deepest Hadal trench sediments. *Geophys. Res. Lett.* 49, e2022GL099365.
- Mackin, J.E., Aller, R.C., 1984. Diagenesis of dissolved aluminum in organic-rich estuarine sediments. *Geochem. Cosmochim. Acta* 48, 299–313.
- Maldonado, M., López-Acosta, M., Sitjà, C., García-Puig, M., Galobart, C., Ercilla, G., Leynaert, A., 2019. Sponge skeletons as an important sink of silicon in the global oceans. *Nat. Geosci.* 12 (10), 815–822.
- Maliva, R.G., Knoll, A.H., Siever, R., 1989. Secular change in chert distribution; a reflection of evolving biological participation in the silica cycle. *Palaios* 4, 519–532.
- Marchetti, A., Cassar, N., 2009. Diatom elemental and morphological changes in response to iron limitation: a brief review with potential paleoceanographic applications. *Geobiology* 7, 419–431.
- Marron, A., Cassarino, L., Hatton, J., Curnow, P., Hendry, K.R., 2019. The silicon isotopic composition of choanoflagellates: implications for a mechanistic understanding of isotopic fractionation during biosilicification. *Biogeosciences* 16, 4805–4813.
- Martin-Jezequel, V., Hildebrand, M., Brzezinski, M.A., 2000. Silicon metabolism in diatoms: implications for growth. *J. Phycol.* 36, 821–840.
- Matsumoto, K., Sarmiento, J.L., 2008. A corollary to the silicic acid leakage hypothesis. *Paleoceanography* 23.
- Matsumoto, K., Sarmiento, J.L., Brzezinski, M.A., 2002. Silicic acid leakage from the Southern Ocean: a possible explanation for glacial atmospheric  $\text{pCO}_2$ . *Global Biogeochem. Cycles* 16.
- McManus, J., Hammond, D.E., Berelson, W.M., Kilgore, T.E., Demaster, D.J., Raguenneau, O.G., Collier, R.W., 1995. Early diagenesis of biogenic opal: dissolution rates, kinetics, and paleoceanographic implications. *Deep Sea Res. Part II Top. Stud. Oceanogr.* 42, 871–903.
- Menicucci, A.J., Spero, H.J., Matthews, J., Parikh, S.J., 2017. Influence of exchangeable oxygen on biogenic silica oxygen isotope data. *Chem. Geol.* 466, 710–721.
- Meyerink, S., Ellwood, M.J., Maher, W.A., Strzepek, R., 2017. Iron availability influences silicon isotope fractionation in two Southern Ocean diatoms (*Proboscia inermis* and *Eucampia antarctica*) and a coastal diatom (*Thalassiosira pseudonana*). *Front. Mar. Sci.* 4, 217.
- Meyerink, S.W., Boyd, P.W., Maher, W.A., Milne, A., Strzepek, R., Ellwood, M.J., 2019. Putting the silicon cycle in a bag: field and mesocosm observations of silicon isotope fractionation in subtropical waters east of New Zealand. *Mar. Chem.* 213, 1–12.
- Michalopoulos, P., Aller, R.C., 1995. Rapid clay mineral formation in amazon delta sediments - reverse weathering and oceanic elemental cycles. *Science* 270, 614–617.
- Michalopoulos, P., Aller, R.C., 2004. Early diagenesis of biogenic silica in the Amazon delta: alteration, authigenic clay formation, and storage. *Geochem. Cosmochim. Acta* 68, 1061–1085.
- Michalopoulos, P., Aller, R.C., Reeder, R.J., 2000. Conversion of diatoms to clays during early diagenesis in tropical, continental shelf muds. *Geology* 28, 1095–1098.
- Milligan, A.J., Varela, D.E., Brzezinski, M.A., Morel, F., 2004. Dynamics of silicon metabolism and silicon isotopic discrimination in a marine diatom as a function of  $\text{pCO}_2$ . *Limnol. Oceanogr.* 49, 322–329.
- Mokadem, F., Parkinson, I.J., Hathorne, E.C., Anand, P., Allen, J.T., Burton, K.W., 2015. High-precision radiogenic strontium isotope measurements of the modern and glacial ocean: limits on glacial-interglacial variations in continental weathering. *Earth Planet Sci. Lett.* 415, 111–120.
- Moriceau, B., Goutx, M., Guigue, C., Lee, C., Armstrong, R., Duflos, M., Tamburini, G., Charière, B., Ragueneau, O., 2009. Si-C interactions during degradation of the diatom Skeletonema marinioi. *Deep Sea Res. Part II Top. Stud. Oceanogr.* 56, 1381–1395.
- Morley, D., Leng, M., Mackay, A., Sloane, H., Rioual, P., Battarbee, R., 2004. Cleaning of lake sediment samples for diatom oxygen isotope analysis. *J. Paleolimnol.* 31, 391–401.
- Murata, K., Friedman, I., Gleason, J., 1977. Oxygen isotope relations between diagenetic silica minerals in Monterey Shale, Temblor Range, California. *Am. J. Sci.* 277, 259–272.
- Nantke, C.K.M., Brauer, A., Frings, P.J., Czymzik, M., Hübener, T., Stadmark, J., Dellwig, O., Roeser, P., Conley, D.J., 2021. Human influence on the continental Si budget during the last 4300 years:  $^{83}\text{Si}$  of diatom in varved lake sediments (Tiefer See, NE Germany). *Quat. Sci. Rev.* 258, 106869.
- Nantke, C.K.M., Frings, P.J., Stadmark, J., Czymzik, M., Conley, D.J., 2019. Si cycling in transition zones: a study of Si isotopes and biogenic silica accumulation in the Chesapeake Bay through the Holocene. *Biogeochemistry* 146, 145–170.
- Nelson, D.M., Goering, J.J., 1977. Near-surface silica dissolution in the upwelling region off northwest Africa. *Deep Sea Research* 24, 65–73.
- Nelson, D.M., Goering, J.J., Kilham, S.S., Guillard, R.R.L., 1976. Kinetics of silicic acid uptake and rates of silica dissolution in the marine diatom *Thalassiosira pseudonana*. *J. Phycol.* 12, 246–252.
- Nelson, D.M., Gordon, L.I., 1982. Production and pelagic dissolution of biogenic silica in the Southern Ocean. *Geochem. Cosmochim. Acta* 46, 491–501.
- Nelson, D.M., Tréguer, P., Brzezinski, M.A., Leynaert, A., Quéguiner, B., 1995. Production and dissolution of biogenic silica in the ocean: revised global estimates, comparison with regional data and relationship to biogenic sedimentation. *Global Biogeochem. Cycles* 9, 359–372.
- Ng, H.C., Cassarino, L., Pickering, R.A., Woodward, E.M.S., Hammond, S.J., Hendry, K.R., 2020. Sediment efflux of silicon on the Greenland margin and implications for the marine silicon cycle. *Earth Planet Sci. Lett.* 529, 115877.
- Ng, H.C., Hawkings, J.R., Bertrand, S., Summers, B.A., Sieber, M., Conway, T.M., Freitas, F.S., Ward, J.P., Pryer, H.V., Wadham, J.L., 2022. Benthic dissolved silicon and iron cycling at glaciated Patagonian fjord heads. *Global Biogeochem. Cycles* 36, e2022GB007493.
- Nozaki, Y., Yamamoto, Y., 2001. Radium 228 based nitrate fluxes in the eastern Indian Ocean and the South China Sea and a silicon-induced "alkalinity pump" hypothesis. *Global Biogeochem. Cycles* 15, 555–567.
- Oelze, M., Schüssler, J.A., von Blanckenburg, F., 2016. Mass bias stabilization by Mg doping for Si stable isotope analysis by MC-ICP-MS. *Journal of Analytical Atomic Spectrometry* 31, 2094–2100.
- Oelze, M., von Blanckenburg, F., Bouchez, J., Hoellen, D., Dietzel, M., 2015a. The effect of Al on Si isotope fractionation investigated by silica precipitation experiments. *Chem. Geol.* 397, 94–105.
- Oelze, M., von Blanckenburg, F., Bouchez, J., Hoellen, D., Dietzel, M., 2015b. The effect of Al on Si isotope fractionation investigated by silica precipitation experiments. *Chem. Geol.* 397, 94.
- Oelze, M., von Blanckenburg, F., Bouchez, J., Hoellen, D., Dietzel, M., 2015c. The effect of Al on Si isotope fractionation during adsorption and the competition between kinetic and equilibrium isotope fractionation: implications for weathering systems. *Chem. Geol.* 380, 161–171.
- Opfergelt, S., Burton, K.W., Pogge von Strandmann, P.A.E., Gislason, S.R., Halliday, A.N., 2013. Riverine silicon isotope variations in glaciated basaltic terrains: implications for the Si delivery to the ocean over glacial-interglacial intervals. *Earth Planet Sci. Lett.* 369–370, 211–219.
- Opfergelt, S., Bourdonville, G., Cardinal, D., André, L., Delstanche, S., Delvaux, B., 2009. Impact of soil weathering degree on silicon isotopic fractionation during adsorption onto iron oxides in basaltic ash soils, Cameroon. *Geochem. Cosmochim. Acta* 73, 7226–7240.

- Opfergelt, S., Eiriksdottir, E., Burton, K., Einarsson, A., Siebert, C., Gislason, S., Halliday, A., 2011. Quantifying the impact of freshwater diatom productivity on silicon isotopes and silicon fluxes: lake Myvatn, Iceland. *Earth Planet Sci. Lett.* 305, 73–82.
- Pack, A., Bultmann, E.-M., Tatzel, M., Reitner, J., 2023. A new method for silicon triple isotope analysis with application to siliceous sponge spicules. *G-cubed* 24, e2023GC011243.
- Panizzo, V., Crespin, J., Crosta, X., Shemesh, A., Massé, G., Yam, R., Mattielli, N., Cardinal, D., 2014. Sea ice diatom contributions to Holocene nutrient utilization in East Antarctica. *Paleoceanography* 29, 328–343.
- Panizzo, V., Swann, G., Mackay, A.W., Pashley, V., Horstwood, M.S., 2018a. Modelling silicon supply during the Last Interglacial (MIS 5e) at Lake Baikal. *Quat. Sci. Rev.* 190, 114–122.
- Panizzo, V.N., Roberts, S., Swann, G.E.A., McGowan, S., Mackay, A.W., Vologina, E., Pashley, V., Horstwood, M.S.A., 2018b. Spatial differences in dissolved silicon utilization in Lake Baikal, Siberia: examining the impact of high diatom biomass events and eutrophication. *Limnol. Oceanogr.* 63, 1562–1578.
- Panizzo, V.N., Swann, G.E.A., Mackay, A.W., Vologina, E., Alleman, L., André, L., Pashley, V.H., Horstwood, M.S.A., 2017. Constraining modern-day silicon cycling in Lake Baikal. *Global Biogeochem. Cycles* 31, 556–574.
- Panizzo, V.N., Swann, G.E.A., Mackay, A.W., Vologina, E., Sturm, M., Pashley, V., Horstwood, M.S.A., 2016. Insights into the transfer of silicon isotopes into the sediment record. *Biogeosciences* 13, 147–157.
- Pedersen, T.F., Francois, R., Francois, L., Alverson, K.D., McManus, J.F., 2003. The late quaternary history of biogeochemical cycling of carbon. In: Alverson, K.D., Bradley, R.S., Pedersen, T.F. (Eds.), *Palaeoclimate, Global Change, and the Future*. Springer-Verlag, Berlin.
- Pichevin, L.E., Ganeshram, R.S., Dumont, M., 2020. Deglacial Si remobilisation from the deep-ocean reveals biogeochemical and physical controls on glacial atmospheric CO<sub>2</sub> levels. *Earth Planet Sci. Lett.* 543, 116332.
- Pichevin, L.E., Ganeshram, R.S., Geibert, W., Thunell, R., Hinton, R., 2014. Silica burial enhanced by iron limitation in oceanic upwelling margins. *Nat. Geosci.* 7, 541–546.
- Pickering, R.A., Cassarino, L., Hendry, K.R., Wang, X.L., Maiti, K., Krause, J.W., 2020. Using stable isotopes to disentangle marine sedimentary signals in reactive silicon pools. *Geophys. Res. Lett.* 47, e2020GL087877.
- Pike, J., Allen, C.S., Leventer, A., Stickley, C.E., Pudsey, C.J., 2008. Comparison of contemporary and fossil diatom assemblages from the western Antarctic Peninsula shelf. *Mar. Micropaleontol.* 67, 274–287.
- Pisciotta, K.A., 1981. Diagenetic trends in the siliceous facies of the monterey shale in the santa maria region, California. *Sedimentology* 28, 547–571.
- Pokharel, R., Gerrits, R., Schulessier, J.A., von Blanckenburg, F., 2019. Mechanisms of olivine dissolution by rock-inhabiting fungi explored using magnesium stable isotopes. *Chem. Geol.* 525, 18–27.
- Presti, M., Michalopoulos, P., 2008. Estimating the contribution of the authigenic mineral component to the long-term reactive silica accumulation on the western shelf of the Mississippi River Delta. *Cont. Shelf Res.* 28, 823–838.
- Rabouille, C., Gaillard, J.-F., Tréguer, P., Vincendeau, M.-A., 1997. Biogenic silica recycling in surficial sediments across the polar front of the Southern Ocean (Indian sector). *Deep Sea Res. Part II Top. Stud. Oceanogr.* 44, 1151–1176.
- Rahman, S., Aller, R., Cochran, J., 2017. The missing silica sink: revisiting the marine sedimentary Si cycle using cosmogenic <sup>32</sup>Si. *Global Biogeochem. Cycles* 31, 1559–1578.
- Rahman, S., Trower, E.J., 2023. Probing surface Earth reactive silica cycling using stable Si isotopes: mass balance, fluxes, and deep time implications. *Sci. Adv.* 9, eadi2440.
- Renaudie, J., 2016. Quantifying the Cenozoic marine diatom deposition history: links to the C and Si cycles. *Biogeosciences Discuss* 2016, 1–17.
- Reynolds, B.C., Aggarwal, J., Andre, L., Baxter, D., Beucher, C., Brzezinski, M.A., Engstrom, E., Georg, R.B., Land, M., Leng, M.J., Opfergelt, S., Rodushkin, I., Sloane, H.J., van den Boorn, S., Vroon, P.Z., Cardinal, D., 2007. An inter-laboratory comparison of Si isotope reference materials. *Journal of Analytical Atomic Spectrometry* 22, 561–568.
- Reynolds, B.C., Frank, M., Halliday, A.N., 2006. Silicon isotope fractionation during nutrient utilization in the North Pacific. *Earth Planet Sci. Lett.* 244, 431–443.
- Richter, F.M., Turekian, K.K., 1993. Simple models for the geochemical response of the ocean to climatic and tectonic forcing. *Earth Planet Sci. Lett.* 119, 121–131.
- Rickert, D., Schlüter, M., Wallmann, K., 2002. Dissolution kinetics of biogenic silica from the water column to the sediments. *Geochim. Cosmochim. Acta* 66, 439–455.
- Rimstidt, J.D., Barnes, H.L., 1980. The kinetics of silica-water reactions. *Geochim. Cosmochim. Acta* 44, 1683–1699.
- Rings, A., Lücke, A., Schleser, G.H., 2004. A new method for the quantitative separation of diatom frustules from lake sediments. *Limnol. Oceanogr. Methods* 2, 25–34.
- Roerdink, D.L., van den Boorn, S.H., Geilert, S., Vroon, P.Z., van Bergen, M.J., 2015. Experimental constraints on kinetic and equilibrium silicon isotope fractionation during the formation of non-biogenic chert deposits. *Chem. Geol.* 402, 40–51.
- Schmidtbauer, K., Noble, P., Rosen, M., Conley, D.J., Frings, P.J., 2022. Linking silicon isotopic signatures with diatom communities. *Geochim. Cosmochim. Acta* 323, 102–122.
- Sharp, Z., Gibbons, J., Maltsev, O., Atudorei, V., Pack, A., Sengupta, S., Shock, E., Knauth, L., 2016. A calibration of the triple oxygen isotope fractionation in the SiO<sub>2</sub>-H<sub>2</sub>O system and applications to natural samples. *Geochim. Cosmochim. Acta* 186, 105–119.
- Shemesh, A., Burckle, L.H., Hays, J.D., 1995. Late Pleistocene oxygen isotope records of biogenic silica from the Atlantic sector of the Southern Ocean. *Paleoceanography* 10, 179–196.
- Shemesh, A., Mortlock, R.A., Smith, R.J., Froelich, P.N., 1988. Determination of Ge/Si in marine siliceous microfossils: separation, cleaning and dissolution of diatoms and radiolaria. *Mar. Chem.* 25, 305–323.
- Sigman, D.M., Boyle, E.A., 2000. Glacial/interglacial variations in atmospheric carbon dioxide. *Nature* 407, 859–869.
- Singh, S.P., Singh, S.K., Bhushan, R., Rai, V.K., 2015. Dissolved silicon and its isotopes in the water column of the Bay of Bengal: internal cycling versus lateral transport. *Geochim. Cosmochim. Acta* 151, 172–191.
- Sjöberg, S., 1996. Silica in aqueous environments. *J. Non-Cryst. Solids* 196, 51–57.
- Snelling, A.M., Swann, G.E., Leng, M.J., Pike, J., 2013. A micro-manipulation technique for the purification of diatoms for isotope and geochemical analysis. *Silicon* 5, 13–17.
- Snelling, A.M., Swann, G.E.A., Pashley, V., Lacey, J.H., Horstwood, M.S.A., Leng, M.J., 2022. Nutrient availability in the North Pacific region not primarily driven by climate through the Quaternary. *Palaeogeogr. Palaeoclimatol. Palaeoecol.* 601, 111109.
- Sommer, U., 1985. Seasonal succession of phytoplankton in lake constance. *Bioscience* 35, 351–357.
- Stamm, F.M., Pickering, R.A., Frings, P.J., Frick, D.A., Richoz, S., Conley, D.J., submitted. Impact of diagenesis on biogenic silica- structural, chemical and isotope proxies. *J. Geophys. Res.: Biogeosciences*.
- Stamm, F.M., Zambardi, T., Chmeleff, J., Schott, J., von Blanckenburg, F., Oelkers, E.H., 2019. The experimental determination of equilibrium Si isotope fractionation factors among H<sub>4</sub>SiO<sub>4</sub>, H<sub>3</sub>SiO<sub>4</sub>- and amorphous silica (SiO<sub>2</sub>-0.32 H<sub>2</sub>O) at 25 and 75 °C using the three-isotope method. *Geochim. Cosmochim. Acta* 255, 49–68.
- Stoll, H.M., Shimizu, N., 2009. Micropicking of nanofossils in preparation for analysis by secondary ion mass spectrometry. *Nat. Protoc.* 4, 1038–1043.
- Street-Perrott, F.A., Barker, P.A., 2008. Biogenic silica: a neglected component of the coupled global continental biogeochemical cycles of carbon and silicon. *Earth Surf. Process. Landforms* 33, 1436–1457.
- Street-Perrott, F.A., Barker, P.A., Leng, M.J., Sloane, H.J., Wooller, M.J., Ficken, K.J., Swain, D.L., 2008. Towards an understanding of late Quaternary variations in the continental biogeochemical cycle of silicon: multi-isotope and sediment-flux data for Lake Rutundu, Mt Kenya, East Africa, since 38 ka BP. *J. Quat. Sci.* 23, 375–387.
- Struyf, E., Conley, D.J., 2009. Silica: an essential nutrient in wetland biogeochemistry. *Front. Ecol. Environ.* 7, 88–94.
- Struyf, E., Smis, A., Van Damme, S., Garnier, J., Govers, G., Van Wesemael, B., Conley, D.J., Batelaan, O., Frot, E., Clymans, W., Vandevenne, F., Lancelot, C., Goos, P., Meire, P., 2010. Historical land use change has lowered terrestrial silica mobilization. *Nat. Commun.* 1, 129.
- Studer, A.S., Ellis, K.K., Oleynik, S., Sigman, D.M., Haug, G.H., 2013. Size-specific opal-bound nitrogen isotope measurements in North Pacific sediments. *Geochim. Cosmochim. Acta* 120, 179–194.
- Sun, H., Chaussidon, M., Robert, F., Tian, S., Deng, Z., Moynier, F., 2023. Triple silicon isotope insights into the formation of Precambrian cherts. *Earth Planet Sci. Lett.* 607, 118069.
- Sun, X., Andersson, P.S., Humborg, C., Pastuszak, M., Mört, C.-M., 2013. Silicon isotope enrichment in diatoms during nutrient-limited blooms in a eutrophied river system. *J. Geochim. Explor.* 132, 173–180.
- Sun, X., Mört, C.-M., Porcelli, D., Kutschler, L., Hirst, C., Murphy, M.J., Maximov, T., Petrov, R.E., Humborg, C., Schmitt, M., 2018. Stable silicon isotopic compositions of the Lena River and its tributaries: implications for silicon delivery to the Arctic Ocean. *Geochim. Cosmochim. Acta* 241, 120–133.
- Sun, X., Olofsson, M., Andersson, P.S., Fry, B., Legrand, C., Humborg, C., Mört, C.-M., 2014. Effects of growth and dissolution on the fractionation of silicon isotopes by estuarine diatoms. *Geochim. Cosmochim. Acta* 130, 156–166.
- Sutton, J.N., André, L., Cardinal, D., Conley, D.J., de Souza, G., Dean, J., Dodd, J., Ehler, C., Ellwood, M.J., Frings, P.J., Grasse, P., Hendry, K.R., Leng, M.J., Michalopoulos, P., Panizzo, V.N., Swann, G.E.A., 2018a. A review of the stable isotope bio-geochemistry of the global silicon cycle and its associated trace elements. *Front. Earth Sci.* 5, 112.
- Sutton, J.N., De Souza, G.F., García-Ibáñez, M.I., De La Rocha, C.L., 2018b. The silicon stable isotope distribution along the GEVIDE section (GEOTRACES GA-01) of the North Atlantic Ocean. *Biogeosciences* 15, 5663–5676.
- Sutton, J.N., Varela, D.E., Brzezinski, M.A., Beucher, C.P., 2013. Species-dependent silicon isotope fractionation by marine diatoms. *Geochim. Cosmochim. Acta* 104, 300–309.
- Swann, G.E., Snelling, A.M., 2023. Isotope sample preparation of diatoms for paleoenvironmental research. *PLoS One* 18, e0281511.
- Swann, G.E.A., Leng, M.J., Juschus, O., Melles, M., Brigham-Grette, J., Sloane, H.J., 2010. A combined oxygen and silicon diatom isotope record of Late Quaternary change in Lake El gygytgyn, North East Siberia. *Quat. Sci. Rev.* 29, 774–786.
- Swann, G.E.A., Patwardhan, S.V., 2011. Application of Fourier Transform Infrared Spectroscopy (FTIR) for assessing biogenic silica sample purity in geochemical analyses and palaeoenvironmental research. *Clim. Past* 7, 65–74.
- Swann, G.E.A., Pike, J., Snelling, A.M., Leng, M.J., Williams, M.C., 2013. Seasonally resolved diatom δ<sub>18</sub>O records from the West Antarctic Peninsula over the last deglaciation. *Earth Planet Sci. Lett.* 364, 12–23.
- Swann, G.E.A., Snelling, A.M., Pike, J., 2016. Biogeochemical cycling in the bering sea over the onset of major northern hemisphere glaciation. *Paleoceanography* 31, 1261–1269.
- Takeda, S., 1998. Influence of iron availability on nutrient consumption ratio of diatoms in oceanic waters. *Nature* 393, 774–777.
- Tatzel, M., Frings, P.J., Oelze, M., Herwartz, D., Lünsdorf, N.K., Wiedenbeck, M., 2022. Chert Oxygen Isotope Ratios Are Driven by Earth's Thermal Evolution, vol. 119. *Proceedings of the National Academy of Sciences*, e2213076119.

- Tatzel, M., Oelze, M., Frick, D.A., Di Rocco, T., Liesegang, M., Stuff, M., Wiedenbeck, M., 2024. Silicon and oxygen isotope fractionation in a silicified carbonate rock. *Chem. Geol.* 122120.
- Tatzel, M., von Blanckenburg, F., Oelze, M., Schuessler, J.A., Bohrmann, G., 2015. The silicon isotope record of early silica diagenesis. *Earth Planet Sci. Lett.* 428, 293–303.
- Tesson, B., Genet, M.J., Fernandez, V., Degand, S., Rouxhet, P.G., Martin-Jézéquel, V., 2009. Surface chemical composition of diatoms. *Chembiochem* 10, 2011–2024.
- Tian, Q., Liu, D., Li, M., Yuan, P., Zhou, J., Guo, H., 2023. Increasing iron concentration inhibits the Al-incorporation into the diatom biogenic silica: from laboratory simulation of ocean iron fertilization. *Chem. Geol.* 639, 121713.
- Tian, Q., Liu, D., Yuan, P., Li, M., Yang, W., Zhou, J., Wei, H., Zhou, J., Guo, H., 2022. Occurrence of structural aluminium (Al) in marine diatom biological silica: visible evidence from microscopic analysis. *Ocean Sci.* 18, 321–329.
- Trégouer, P., Kamatani, A., Gueneley, S., Quéguiner, B., 1989. Kinetics of dissolution of Antarctic diatom frustules and the biogeochemical cycle of silicon in the Southern Ocean. *Polar Biol.* 9, 397–403.
- Trégouer, P.J., Sutton, J.N., Brzezinski, M., Charette, M.A., Devries, T., Dutkiewicz, S., Ehlers, C., Hawkings, J., Leynaert, A., Liu, S.M., Llopis Monferrer, N., López-Acosta, M., Maldonado, M., Rahman, S., Ran, L., Rouxel, O., 2021. Reviews and syntheses: the biogeochemical cycle of silicon in the modern ocean. *Biogeosciences* 18, 1269–1289.
- Truesdale, V.W., Greenwood, J.E., Rendell, A., 2005. The rate-equation for biogenic silica dissolution in seawater – new hypotheses. *Aquat. Geochem.* 11, 319–343.
- Tyler, J.J., Sloane, H.J., Rickaby, R.E., Cox, E.J., Leng, M.J., 2017. Post-mortem oxygen isotope exchange within cultured diatom silica. *Rapid Commun. Mass Spectrom.* 31, 1749–1760.
- Van Bennekom, A.J., Buma, A.G.J., Nolting, R.F., 1991. Dissolved aluminium in the Weddell-Scotia Confluence and effect of Al on the dissolution kinetics of biogenic silica. *Mar. Chem.* 35, 423–434.
- van Bennekom, A.J., Fred Jansen, J.H., van der Gaast, S.J., van Iperen, J.M., Pieters, J., 1989. Aluminium-rich opal: an intermediate in the preservation of biogenic silica in the Zaire (Congo) deep-sea fan. *Deep-Sea Res., Part A* 36, 173–190.
- Van Beusekom, J., Van Bennekom, A., Trégouer, P., Morvan, J., 1997. Aluminium and silicic acid in water and sediments of the Enderby and Crozet Basins. *Deep Sea Res. Part II Top. Stud. Oceanogr.* 44, 987–1003.
- Van Cappellen, P., Dixit, S., van Beusekom, J., 2002. Biogenic silica dissolution in the oceans: reconciling experimental and field-based dissolution rates. *Global Biogeochem. Cycles* 16, 23, 21–23–10.
- Van Cappellen, P., Qiu, L., 1997a. Biogenic silica dissolution in sediments of the Southern Ocean. I. Solubility. *Deep Sea Res. Part II Top. Stud. Oceanogr.* 44, 1109–1128.
- Van Cappellen, P., Qiu, L., 1997b. Biogenic silica dissolution in sediments of the Southern Ocean. II. Kinetics. *Deep Sea Res. Part II Top. Stud. Oceanogr.* 44, 1129–1149.
- van Tol, H.M., Irwin, A.J., Finkel, Z.V., 2012. Macroevolutionary trends in silicoflagellate skeletal morphology: the costs and benefits of silification. *Paleobiology* 38, 391–402.
- Vance, D., Little, Susan H., de Souza, Gregory F., Khatiwala, S., Lohan, Maeve C., Middag, R., 2017. Silicon and zinc biogeochemical cycles coupled through the Southern Ocean. *Nat. Geosci.* 10, 202.
- Varela, D., Brzezinski, M., Beucher, C., Jones, J., Giesbrecht, K., Lansard, B., Mucci, A., 2016. Heavy silicon isotopic composition of silicic acid and biogenic silica in Arctic waters over the Beaufort shelf and the Canada Basin. *Global Biogeochem. Cycles* 30, 804–824.
- Varela, D.E., Pride, C.J., Brzezinski, M.A., 2004. Biological fractionation of silicon isotopes in Southern Ocean surface waters. *Global Biogeochem. Cycles* 18.
- Wallace, A.F., Wang, D., Hamm, L.M., Knoll, A.H., Dove, P.M., 2012. Eukaryotic skeletal formation. In: Knoll, A.H., Canfield, D.E., Konhauser, K.O. (Eds.), *Fundamentals of Geobiology*. John Wiley & Sons, Ltd, Chichester, pp. 150–187.
- Ward, J.P.J., Hendry, K.R., Arndt, S., Faust, J.C., Freitas, F.S., Henley, S.F., Krause, J.W., März, C., Ng, H.C., Pickering, R.A., Tessin, A.C., 2022a. Stable silicon isotopes uncover a mineralogical control on the benthic silicon cycle in the Arctic Barents Sea. *Geochim. Cosmochim. Acta* 329, 206–230.
- Ward, J.P.J., Hendry, K.R., Arndt, S., Faust, J.C., Freitas, F.S., Henley, S.F., Krause, J.W., März, C., Tessin, A.C., Airs, R.L., 2022b. Benthic silicon cycling in the Arctic Barents Sea: a reaction-transport model study. *Biogeosciences* 19, 3445–3467.
- Weiss, A., De La Rocha, C., Amann, T., Hartmann, J., 2015. Silicon isotope composition of dissolved silica in surface waters of the Elbe Estuary and its tidal marshes. *Biogeochemistry* 1–19.
- Weiss, D.J., Boye, K., Caldelas, C., Fendorf, S., 2014. Zinc isotope fractionation during early dissolution of biotite granite. *Soil Sci. Soc. Am. J.* 78, 171–179.
- Wetzel, F., de Souza, G.F., Reynolds, B.C., 2014. What controls silicon isotope fractionation during dissolution of diatom opal? *Geochem. Cosmochim. Acta* 131, 128–137.
- Wille, M., Sutton, J., Ellwood, M.J., Cambridge, M., Maher, W., Eggins, S., Kelly, M., 2010a. Silicon isotopic fractionation in marine sponges: a new model for understanding silicon isotopic variations in sponges. *Earth Planet Sci. Lett.* 292, 281–289.
- Wille, M., Sutton, J., Ellwood, M.J., Cambridge, M., Maher, W., Eggins, S., Kelly, M., 2010b. Silicon isotopic fractionation in marine sponges: a new model for understanding silicon isotopic variations in sponges. *Earth Planet Sci. Lett.* 292, 281.
- Williams, L.A., Crerar, D.A., 1985. Silica diagenesis, II. General mechanisms. *J. Sediment. Res.* 55.
- Williams, L.A., Parks, G.A., Crerar, D.A., 1985. Silica diagenesis .1. Solubility controls. *J. Sediment. Petrol.* 55, 301–311.
- Wollast, R., 1974. The silica problems. *The sea* 5, 359–392.
- Worrell, S., Swann, G.E.A., Kender, S., Lacey, J.H., Leng, M.J., 2022. Silicic acid cycling in the bering sea during the mid-pleistocene transition. *Paleoceanogr. Paleoclimatol.* 37, e2021PA004284.
- Wu, B., Lu, C., Liu, S., 2015. Dynamics of biogenic silica dissolution in jiaozhou Bay, western yellow sea. *Mar. Chem.* 174, 58–66.
- Xiang, L., Huang, X., Sun, M., Panizzo, V.N., Huang, C., Zheng, M., Chen, X., Chen, F., 2023. Prehistoric population expansion in central asia promoted by the Altai Holocene climatic optimum. *Nat. Commun.* 14, 3102.
- Yamoah, K.A., Callac, N., Chi Fru, E., Wohlfarth, B., Wiech, A., Chabangborn, A., Smittenberg, R.H., 2016. A 150-year record of phytoplankton community succession controlled by hydroclimatic variability in a tropical lake. *Biogeosciences* 13, 3971–3980.
- Yanchilina, A.G., Yam, R., Kolodny, Y., Shemesh, A., 2020. From diatom opal-A 8180 to chert 8180 in deep sea sediments. *Geochem. Cosmochim. Acta* 268, 368–382.
- Yanchilina, A.G., Yam, R., Shemesh, A., 2021. The effect of sediment lithology on oxygen isotope composition and phase transformation of marine biogenic opal. *Chem. Geol.* 570, 120175.
- Ye, Y., Frings, P.J., von Blanckenburg, F., Feng, Q., 2021. Silicon isotopes reveal a decline in oceanic dissolved silicon driven by biosilicification: a prerequisite for the Cambrian Explosion? *Earth Planet Sci. Lett.* 566, 116959.
- Zahajská, P., Frings, P.J., Gaspard, F., Opfergelt, S., Stadmark, J., Fritz, S.C., Cartier, R., Conley, D.J., 2023. The Holocene silicon biogeochemistry of Yellowstone Lake, USA. *Quat. Sci. Rev.* 322, 108419.
- Zahajská, P., Olid, C., Stadmark, J., Fritz, S.C., Opfergelt, S., Conley, D.J., 2021. Modern silicon dynamics of a small high-latitude subarctic lake. *Biogeosciences* 18, 2325–2345.
- Zhang, A., Zhang, J., Hu, J., Zhang, R., Zhang, G., 2015. Silicon isotopic chemistry in the Changjiang Estuary and coastal regions: impacts of physical and biogeochemical processes on the transport of riverine dissolved silica. *J. Geophys. Res.: Oceans* 120, 6943–6957.
- Zhang, Z., Sun, X., Dai, M., Cao, Z., Fontorbe, G., Conley, D.J., 2020. Impact of human disturbance on the biogeochemical silicon cycle in a coastal sea revealed by silicon isotopes. *Limnol. Oceanogr.* 65, 515–528.
- Zheng, X.-Y., Beard, B.L., Johnson, C.M., 2019. Constraining silicon isotope exchange kinetics and fractionation between aqueous and amorphous Si at room temperature. *Geochem. Cosmochim. Acta* 253, 267–289.
- Zheng, X.-Y., Beard, B.L., Reddy, T.R., Roden, E.E., Johnson, C.M., 2016. Abiologic silicon isotope fractionation between aqueous Si and Fe(III)-Si gel in simulated Archean seawater: implications for Si isotope records in Precambrian sedimentary rocks. *Geochem. Cosmochim. Acta* 187, 102–122.
- Ziegler, K., Chadwick, O.A., Brzezinski, M.A., Kelly, E.F., 2005. Natural variations of  $\delta^{28}\text{Si}$  ratios during progressive basalt weathering, Hawaiian Islands. *Geochem. Cosmochim. Acta* 69, 4597–4610.